

## CHAPTER - II

### SYNTHESIS AND CHARACTERISATION OF POLYESTERS

---

#### 2.1 INTRODUCTION

Carothers was the first to stimulate the work on step growth polymerisation reactions to synthesise aliphatic polyesters originating from dicids and diols based on the theories of Staudinger. Observations at the early stages limited the applications of these linear aliphatic polyesters due to its low glass transition temperatures ( $T_g$ ), low melting points ( $T_m$ ), ease of solubility, and sensitivity to hydrolysis. Later the introduction of aromatic terephtholyl group by Whinfield and Dickson in the beginning of 1940s led to the semi crystalline polyesters with a huge success which is one of the most commercial polymer namely poly(ethylene terephthalate) (PET). In recent years, polyesters has deserved its position uniquely due to its desirable properties including high tensile strength, dimensional stability, chemical and environmental resistance thereby making it an excellent candidate for a variety of potential applications from ancient packing to emerging biomaterials<sup>1</sup>. Retaining its usage forever has been additionally credited as it enters in moulding the life securing system like artificial knee caps, hip joints, bone screws, implantation, bone replacement, drug delivery systems, tissue engineering<sup>2-4</sup> which has remarkably boosted the polyesters. Though it has synthetic versatility, most of the factors influence the course of the reaction including ring size, substituents effect, type of initiator, catalyst, solvent, concentration, temperature and possible trans esterification reactions i.e., back biting or end to end biting. However the extent of degradation generally proceeds via hydrolysis of main chain ester bonds<sup>5,6</sup> where the polymer intrudes, disperse and swell in water resulting in the modification of physical properties in the form of gelation, thickening or by emulsification. Unfortunately most of the synthetic polymers lack reactive functional sites such as  $-NH_2$ ,  $-COOH$  or  $-OH$  which is essential to elicit different interactions and to tune its physico-chemical characteristics. Besides its fleeting applications, the challenge is to find the ultimate polymer that can replace existing materials without environmental foot prints. Thus significant effort has been extended to overcome these limitations in order to facilitate a facile synthesis towards a broad spectrum of applications.

##### 2.1.1 Aliphatic to aromatic polyesters- A systematic approach

The development of biodegradable aliphatic and aromatic polyesters has promising future with low product cost and excellent properties. It incorporates sufficient economic benefits with low priced monomer such as butanediol, adipic acid and terephthalic acid as a starting material. Aliphatic polyesters obtained by the combination of diols and dicarboxylic acids are biodegradable and sensitive to hydrolysis, but lacks improved thermal and mechanical stability which is a key initiator for vast applications. Its low melting point, glass transition temperature and poor hydrolytic stability makes it low-molecular-weight plasticizers. Few aliphatic polyesters known for their biodegradability and biocompatibility possess the tendency to get blended with commercial polymers. Expanding the applications is possible on increasing the glass transition temperature, mechanical property as well as dimensional stability. In order to quench this drawback, research efforts towards aromatic polyesters has been made using various approaches.

Aromatic polyesters have an excellent pattern of physical properties being strongly resistant to hydrolysis, bacterial and fungal attack<sup>7</sup> but can be degraded when they get copolymerised with aliphatic polyesters. Its high crystallinity enables its synthesis in a complicated pathway. On the other hand, its incorporated broad array of properties like high softening points (480 K - 630 K), good dielectric strength, excellent mechanical properties and good heat resistance makes it an essential component for potential applications. When aromatic monomer groups are introduced into the main chain of aliphatic polyesters, undoubtedly the mechanical properties<sup>8-11</sup> are enhanced thereby increasing the rigidity of polymeric backbone with limited chain motion and improved glass transition temperature. However, this often elevates the melting temperature. As an additive credit it enhances good resistance to hydrolysis and chemical agents making the material stiffer with less elongation and less microbial degradation with the environmental circumstances<sup>12</sup>. Depending on the structural chain design the aliphatic and aromatic polyesters can be classified under the cluster of linear and branched grades. Linearity in structure gives a foot print of clarity, adhesion properties and low stiffness, whereas the branching stiffens the polymeric backbone making it more rigid. Thus the present discussion is to fleet with the synthesis of aromatic and aliphatic polyesters which has been framed based on the review made as represented below.

### **2.1.2 Review of literature**

**Matteo Gigli *et al.***, aimed to provide an overview on the use of poly (butylene succinate) (PBS) and its copolymers due to its interesting thermo-mechanical properties, biodegradability, and low production costs. Biodegradation rate and biocompatibility of PBS

class of polyesters which is a bio based polymer were compared and reported along with its envisioned applications<sup>13</sup>.

**Vasilios Tsanaktsis *et al.***, utilised 2,5-furan dicarboxylic acid (2,5-FDCA) and aliphatic diols containing 5 and 7 intervening methylene units to synthesise novel poly (pentylene furanoate) (PPeF) and poly(heptylene furanoate) (PHepF). The polyesters synthesised via polycondensation method were characterised and its thermal properties were also dealt in detail<sup>14</sup>.

**Xiaochuan Ma *et al.***, investigated a series of aromatic polyesters whose bulky propeller-like triphenylamine led to a good solubility in organic solvents and its fabrication into films was facilitated by spin- or inject-coating due to its butterfly-like conformation of phenothiazine. Its potential applications as photoelectrical material was evident from its thermal stability of 10% weight loss at 420 °C, fluorescence nature at 522 nm as well as calculated HOMO and LUMO energy levels<sup>15</sup>.

**Benjamin Nottelet *et al.***, combined biomaterials and contrast agents (CAs)/imaging probes (IPs) for theranostic and diagnostic applications. Investigations related to the modifications of polyester back bones in order to yield macromolecular imaging agents was done and its application in cell labelling and medical field was analysed<sup>16</sup>.

**Ana C. Fonseca *et al.***, synthesised unsaturated polyester resins (UPRs) using synthetic unsaturated polyesters (UPs) with high green content followed by cross linking with 2-hydroxyethyl methacrylate. The synthesised polyesters were characterised with high poly dispersity index, good thermal stability along with well branched structures<sup>17</sup>.

**Julius N. Korley *et al.***, utilised crystalline monomeric form of dihydroxyacetone, a diol to react with diacids containing even numbered methylene moieties like adipic, suberic and sebacic acids in one step without protecting strategies, adopting Schotten – Baumann acylation. Influence of linearity as well as molecular weight of polyesters on physical and thermal properties were dealt<sup>18</sup>.

**George Z. Papageorgiou *et al.***, adopted melt polycondensation method to synthesise bio-based furanic polyester, poly(octylene furanoate). For the first time, temperature modulation (TMDSC) and Fast Scanning Calorimetry (FSC) approaches were made followed by optical microscopic examination by which the size elicited was less than 10 µm<sup>19</sup>.

**Grazia Totaro *et al.***, evaluated antimicrobial activity of newly synthesised Ricinoleic acid and 10-undecenoic acid from castor oil. An approach to link molecules with double bonds of PRA and undeconate units along with insertion of new functionalities was studied in detail<sup>20</sup>.

**Ayumi Tanaka *et al.***, applied lipase-catalysed polycondensation between diols and dimethyl mercaptosuccinate to synthesise reversibly crosslinked aliphatic and aromatic polyesters with free pendant mercapto groups. Its physico chemical properties were analysed along with molecular weight determination. It was favoured with high molecular weight of 17000–27000 g mol<sup>-1</sup> in high yields<sup>21</sup>.

**Aqdas Noreen *et al.***, suggested the algal biomass as a renewable resource to synthesise polyesters due to its high growth rate, good photosynthetic efficiency, potential towards carbon dioxide fixation, low percentage of lignin and high amount of carbohydrates. Review report on algal bio-refinery concept and its biodegradable nature towards medicinal field was also documented<sup>22</sup>.

**Danilo Hansen Guimaraes *et al.***, reported the polycondensation between glycerol and phthalic acid in the ratio 2:2; 2:3 and 2:4 using dibutyltin dilaurate. FTIR confirmed the esterification of glycerol. Non-crystallinity was evident from DSC, whereas XRD plots indicated crystalline nature. Homogeneity of the synthesised polymers was supported by scanning electron microscopic analysis<sup>23</sup>.

**Prabha Littis Malar.G.S *et al.***, synthesised biodegradable polyesters (polyols) from sesame oil and its effect towards non-toxic monomers such as citric acid, 1,2-ethanediol, 1,6-hexanediol without addition of catalyst or solvents were studied by thermal poly condensation technique. Synthesised co-polyesters were characterised using FT-IR, <sup>1</sup>H-NMR, TG-DTA, SEM and tested for its solubility and mechanical strength. According to the choice of monomers, polyesters exhibited various degradation strategy and cell affinity<sup>24</sup>.

**Maryam Saleh Mohammadnia *et al.***, used controlled molecular weight method to prepare various polyesters in presence of *p*-toluene sulfonic acid (*p*-TSA) as an efficient catalyst and starting materials as adipic acid, mono / di / triethylene glycol, 2-ethyl-2-(hydroxymethyl) propane-1,3-diol and 1,4-butanediol. Investigation on the effect of catalyst on reaction rate was carried out. The synthesised polyesters was characterised using FT-IR, <sup>1</sup>H-NMR and <sup>13</sup>C –NMR spectroscopy<sup>25</sup>.

**Joy Vasanthi et al.**, synthesised polymers with pendent benzylidene group by condensing diols with benzalaniline 3'-4'-dimethoxy terephthalic acid. UV, IR, NMR and CHNS analysis was carried out for diacid monomer, whereas polyesters were characterised by IR, TGA and for liquid crystalline property. Highest thermal stability up to 335°C along with good solubility and thermal stability was also revealed<sup>26</sup>.

**Angelica Díaz et al.**, reviewed the status concerned with synthesis, biodegradation and applications of a series of polyesters towards hydrogels, soft tissue engineering, drug delivery systems and liquid crystals. Its nature from elasticity to rigidity was also studied. Drastic change in stiffness of molecular chains and intermolecular interactions was achieved by incorporating aromatic units and  $\alpha$ -amino acids. Extensive discussion on natural amino acids (poly(ester amide)s) has also been revealed<sup>27</sup>.

**Indira et al.**, explored the synthesis of novel polyester elastomers namely poly[poly(ethylene glycol) suberate citrate], PPEGSuC and poly[poly(ethylene glycol) sebacate citrate], PPEGSeC, by carrying out catalyst free polycondensation. IR, <sup>1</sup>H NMR, <sup>13</sup>C NMR and DSC spectral characterisation was carried out and its solubility and viscosity was tested. A control on the chemical structure, morphology, surface nature and physical integrity of the synthesised polyesters was studied by varying the monomers<sup>28</sup>.

**Luis Cabrales et al.**, prepared polyesters by melt polycondensation method using sebacic acid, hexane diol and hydroquinone with the plant derived oils and diols. Gel permeation chromatography, X-ray diffraction, Fourier transform infrared spectroscopy were used to analyse the polyesters. Three-bending point flexural test, tensile testing and contact angle measurements were also carried out<sup>29</sup>.

**Ning Li et al.**, successfully synthesised carborane-containing polyesters with high thermostability by catalytic polycondensation. The thermal transition mechanism of carborane-containing polyesters was studied. FTIR analysis was done and higher char yield was revealed from TG-FTIR. The newly prepared high temperature polyesters have enormous technical and economic value and appreciated especially in the high temperature applications<sup>30</sup>.

**Joseph M. Dennis et al.**, synthesised novel polyesters containing hydrogenated naphthalene rings with a thermal stability of 350°C. Compression moulding techniques were used to obtain ductile and optical clear films. High molecular weight was obtained through viscosity measurements. The structure property relationship for glass transition temperatures

( $T_g$ ) and  $\beta$ -relaxations was studied using differential scanning calorimetry and dynamic mechanical analysis<sup>31</sup>.

**Jing Wu *et al.***, utilised melt polymerisation to synthesise bio based polyesters using renewable isohexide blocks. The preserved stereo configurations of the isohexide moieties were confirmed from  $^1\text{H}$ ,  $^{13}\text{C}$  and 2D-COSY NMR techniques and structure – thermal property was studied. It was assured as a promising material for high performance polymers due to its enhanced reactivity, high thermal stability and increased  $T_g$  around 70 and 85 °C<sup>32</sup>.

For the first time, **Thomas J. Farmer *et al.***, synthesised unsaturated polyesters by using bio-derived di-acids and characterised using TGA, DSC, GPC and NMR techniques. Molecular weight of  $M_n$ , 480–477,000 and  $T_g$  of –30.1 to –16.6 °C was also observed<sup>33</sup>.

**Dilek S. enol *et al.***, under argon atmosphere synthesised polyesters involving novel Schiff base and aliphatic dihalogen. The structural analysis of synthesized substances were carried out using FT-IR and NMR spectral analysis. Fluorescence and UV–vis measurements supported optical nature and thermal analysis using TG-DTA and DSC techniques. In addition, electrochemical and electrical conductivity measurements were also carried out. Effect of ester groups on thermal and physical properties were also explored<sup>34</sup>.

**Benarbia Abderrahim *et al.***, synthesised branched polyesters using ethylene glycol, adipic acid and glycerol followed by its characterisation using FTIR,  $^1\text{H}$  NMR,  $^{13}\text{C}$ -NMR, GPC and TGA/DTA. TGA analysis showed the mass loss in two stages. Decreased band intensity at  $\delta = 1170 \text{ cm}^{-1}$  (C–O–C) and decreased ester band group were confirmed by FT-IR<sup>35</sup>.

**Viswanathan Kavimani *et al.***, prepared a new series of polyesters namely poly (sorbitol x-co-diethylene glycol – x) where x= succinate, adipate, suberate and sebacate mainly comprising of diacids, sorbitol and diethylene glycol. FT-IR,  $^1\text{H}$  and  $^{13}\text{C}$  spectral techniques were used to analyse the synthesised polyesters<sup>36</sup>.

**Prabha Littis Malar *et al.***, adopted thermal polycondensation method to synthesise epoxy resin and polyol which were then characterised using NMR and FT-IR spectral analysis. Thermal response was revealed from TG-DTA studies. Additionally SEM analysis and solubility tests were carried out<sup>37</sup>.

**Muhammad Humayun Bilal *et al.***, enzymatically synthesized biodegradable and hydrophilic functional polyesters with pendant – OH groups from their sugar units which were

esterified to different degrees with stearic acid chloride. The structure were characterized by  $^1\text{H}$  NMR SEC, DSC, WAXS and SAXS analysis<sup>38</sup>.

## 2.2 EXPERIMENTAL METHODS

### 2.2.1 Materials

Dicarboxylic acids, glycerol, phenol and cyclohexanone were purchased and used as such without further purification.

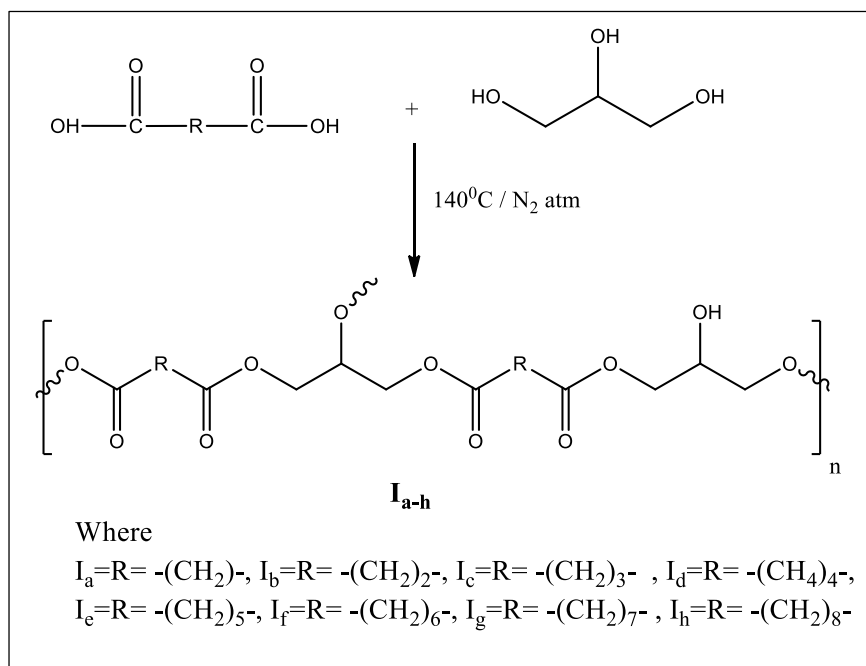
### 2.2.2 Synthesis

#### 2.2.2.1 Synthesis of aliphatic polyesters (I<sub>a-h</sub>)

Classically there are three major routes for the synthesis of aliphatic polyesters as reported in the literature<sup>39-41</sup>

- (i) By the polycondensation of hydroxy acid and diol (or) diacid to obtain the polymer of high molecular weight but never paves the way for block co-polymers.
- (ii) By the ring opening polymerisation (ROP) of lactones and other cyclic diesters such as lactide and glycolide under proper conditions which when improper may lead to racemisation. In addition block co-polymers can be synthesised.
- (iii) By enzymatic polymerisation avoiding the usage of toxic reagents with the possibility to recycle the catalyst but relatively low molecular weight polymers are obtained.

Glycerol is a basic component of lipids and by-product of biodiesel, which is used as monomer with a diacid for the synthesis of polyesters. Thus the present synthesis aims at polymerising glycerol with diacids adopting the **Scheme 1** where polymerisation was initiated by charging a two necked round bottomed flask with the respective dicarboxylic acids (0.1 M) and glycerol (0.1 M) in 1:1 ratio and refluxing it for a specified time at 140°C under the nitrogen atmosphere till the solution became homogeneous. It was further equipped with constant mechanical stirring until a viscous product was obtained<sup>42</sup>. The structure of the synthesised polymers are represented in the **Table 2.1**.



**Scheme 1 Synthesis of aliphatic polyesters**

Detailed description of physical properties of polyesters (I<sub>a-h</sub>) are as follows

I<sub>a</sub>=Poly (Glycerol malonate) (PGM), Yield = 90%, Yellow waxy solid

I<sub>b</sub>=Poly (Glycerol succinate) (PGS), Yield = 85%, colourless waxy solid

I<sub>c</sub>=Poly (Glycerol glutarate) (PGG), Yield = 92%, Brown waxy solid

I<sub>d</sub>=Poly (Glycerol adipate) (PGA), Yield = 85%, Colourless waxy solid

I<sub>e</sub>=Poly (Glycerol pimelate) (PGP), Yield = 90%, Brown waxy solid

I<sub>f</sub>=Poly (Glycerol suberate) (PGSU), Yield = 94%, Pale white waxy solid

I<sub>g</sub>=Poly (Glycerol azealate) (PGAZ), Yield = 90%, Pale brown waxy solid

I<sub>h</sub>=Poly (Glycerol sebaccate) (PGSE), Yield = 95%, Yellow waxy solid

### 2.2.2.2 Synthesis of aromatic (cardo) polyesters (II<sub>a-h</sub>)

The three major process described in the literature for the synthesis of aromatic polyesters are depicted below<sup>43</sup>,

#### (i) Solution polymerisation

This type of polymerisation requires dry solvents, expensive recycling of solvents and expensive acid chlorides. Hydrogen chloride liberated as a by-product of esterification reaction could cause corrosive nature.



## **(ii) Melt polymerisation**

Trans-esterification between diols and diacids require higher temperature to overcome activation energy to proceed in melt polymerisation. Low molecular weight by products can be removed by applying high vacuum which could result in shifting equilibrium towards the formation of high molecular weight polyesters. But viscosity of the reaction medium will prevent the removal of volatile by products which can lead to minimum conversion of reactant into product.

## **(iii) Interfacial polycondensation (IPC)**

Interfacial polycondensation does not require exact 1:1 stoichiometric proportion of the co monomers which can produce high molecular weight polymers than that of melt and solution polymerisation methods. Interfacial polymerisation is an alternate of Schotten–Baumann solution reaction where the reaction is carried out interfacially by means of bisphenol dissolved in aqueous NaOH (base) followed by adding diacyl chlorides in organic solvent which is immiscible in water. The chemistry of this reaction gets facilitated in the presence of phase transfer catalysts where the polymer begins to generate at the interface of two immiscible phases. This method is specifically used for the esterification involving aromatic diols wherein the aliphatic diols will slow down the reaction. It is difficult to get polymers with high molecular weight because of certain substituents which can reduce the basicity of phenoxide ion or sterically hinder the reaction of phenol groups. Mechanism followed in interfacial polycondensation is of diffusion controlled<sup>44</sup>. Beside the factors like solvents, rates of stirring, temperature, phase transfer catalysts and accelerators, presence of phase transfer catalysts facilitates the reaction rate by transferring phenoxide ions into the organic phase.

### **(a) Highlights of interfacial polycondensation**

Among the above mentioned methods, interfacial polycondensation (IPC) has been chosen considering the following merits.

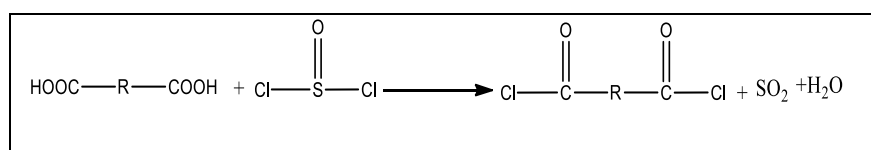
- (i) Interfacial polycondensation is rapid, irreversible, simple to carry out in an open laboratory equipment with or without stirring with a good yield.
- (ii) It is a step growth polymerisation where polymerisation takes place between aqueous solution and organic solution interface containing monomers.

- (iii) Schotten-Baumann reaction mechanism was followed where a diacid chloride of organic phase reacts with monomer containing active hydrogen atoms like -OH, -NH, -SH.
- (iv) Since both the phases are immiscible, reaction rate must be high favouring high molecular weight polymers.
- (v) IPC favours the synthesis of most of the polymers such as polyamides, polyesters, polyurethanes, polysulfonamides and polycarbonates.

In an attempt to synthesize new polyesters by the condensation of aliphatic diacid chloride with aromatic diols, the present work has been undertaken whose frame work consists of three stages.

### Step (i) Synthesis of di-acid chloride

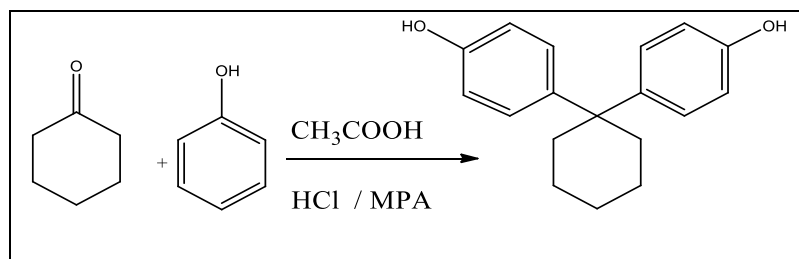
The synthesis was carried out by refluxing the respective dicarboxylic acids with excess thionyl chloride and few drops of pyridine as catalyst. The product obtained was finally washed and recrystallized with n-hexane.



where R =  $-(\text{CH}_2)-$ ,  $-(\text{CH}_2)_2-$ ,  $-(\text{CH}_2)_3-$ ,  $-(\text{CH}_2)_4-$ ,  $-(\text{CH}_2)_5-$ ,  $-(\text{CH}_2)_6-$ ,  $-(\text{CH}_2)_7-$ ,  $-(\text{CH}_2)_8-$

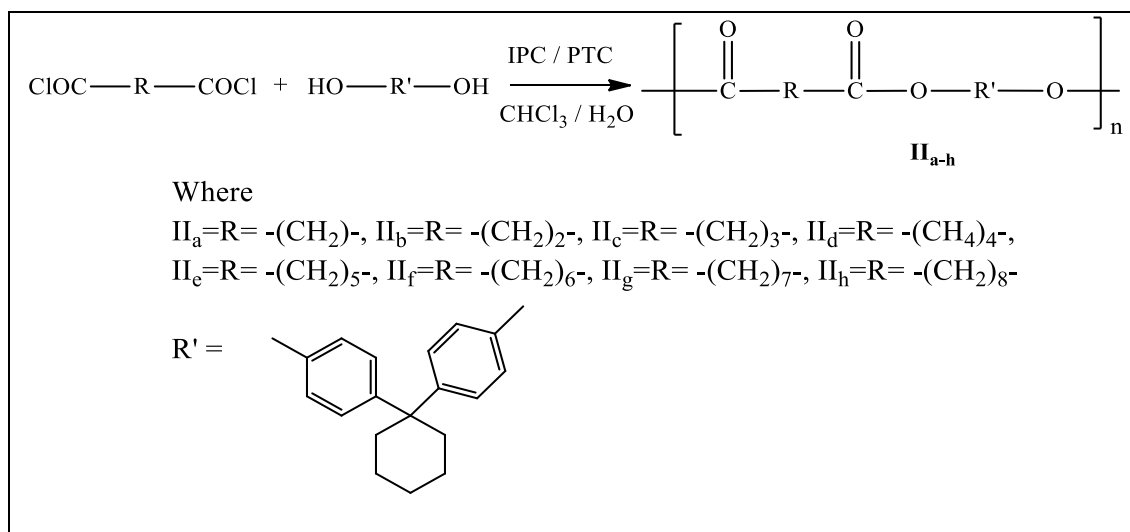
### Step (ii) Synthesis of monomer (bisphenols)

The reaction was initiated by charging 500 ml round bottom flask with cyclohexanone (0.1 M), phenol (1 M) and 3-mercaptopropionic acid (0.01 M) followed by the addition of a mixture of conc. HCl (60 ml) and glacial acetic acid (30 ml). The reaction mixture was stirred gently at ambient temperature for sufficient time. The solid product obtained was further dissolved in ethyl acetate (500 ml) and washed with aqueous sodium bicarbonate solution. Finally the excess solvent was removed on a rotary evaporator followed by distillation under reduced pressure to remove phenol<sup>45</sup>.



### Step (iii) Synthesis of polyester (IPC) (**II** a-h)

About 0.025 M sodium hydroxide dissolved in 75 ml of water was introduced into a 250 ml beaker and placed in a mechanical stirrer with a moderate speed. Further the reaction mixture was added with diol monomer (0.0125 M) and sodium lauryl sulphate (0.25 mg) as phase transfer catalyst. Subsequently, diacid chloride (0.0125 M) in chloroform was added with a maximum stirring rate. After gentle stirring for few minutes, the polymer formed was filtered and washed with acetone to remove unreacted monomers and chloroform. The moist polymerized product was dried under vacuum<sup>46</sup> as outlined below (**Scheme 2**).



### Scheme 2 Synthesis of aromatic polyesters

The structure of the resulting cardo polyesters are predicted in **Table 2.2**. According to the schematic illustration shown in **Scheme 2**, physical properties of cardo polyesters are outlined.

Physical properties of synthesised aromatic polyesters are as follows

$\text{II}_a=4\text{-}(1\text{-}(4\text{-methoxyphenyl})\text{cyclohexyl})\text{phenyl 3-oxobutanoate (MPOB)}$

Yield = 90%, Pale brown solid

$\text{II}_b=4\text{-}(1\text{-}(4\text{-methoxyphenyl})\text{cyclohexyl})\text{phenyl 4-oxopentanoate(MPOP)}$

Yield = 85%, Pale brown solid

$\Pi_c$ =4-(1-(4-methoxyphenyl)cyclohexyl)phenyl 5-oxohexanoate (MPOHX)

Yield = 95%, Pale brown solid

$\Pi_d$ =4-(1-(4-methoxyphenyl)cyclohexyl)phenyl 6-oxoheptanoate (MPOHP)

Yield = 85%, Pale brown solid

$\Pi_e$ =4-(1-(4-methoxyphenyl)cyclohexyl)phenyl 7-oxooctanoate (MPOO)

Yield = 95%, Pale brown solid

$\Pi_f$ =4-(1-(4-methoxyphenyl)cyclohexyl)phenyl 8-oxononanoate (MPON)

Yield = 90%, Pale brown solid

$\Pi_g$ =4-(1-(4-methoxyphenyl)cyclohexyl)phenyl 9-oxodecanoate (MPOD)

Yield = 85%, Pale brown solid

$\Pi_h$ =4-(1-(4-methoxyphenyl)cyclohexyl)phenyl 10-oxoundecanoate (MPOU)

Yield = 80%, Pale brown solid

### **2.2.3 Characterisation techniques**

#### **2.2.3.1 Fourier transform Infra-red spectroscopy (FT-IR)**

FT-IR spectroscopy is a technique based on the vibration of atoms in a molecule associated with a change in dipole moment. The resulting bands in the absorption spectrum corresponds to the frequency of vibration of a part of sample molecule. The most significant information that can be revealed is the presence of functional groups. In the present study, FT-IR spectra of the polymers were recorded using ATR-FTIR-IR of Shimadzu in the frequency range of 4000-400  $\text{cm}^{-1}$ .

#### **2.2.3.2 $^1\text{H}$ and $^{13}\text{C}$ Nuclear magnetic resonance spectroscopy (NMR)**

Proton ( $^1\text{H}$ ) and carbon ( $^{13}\text{C}$ ) NMR were recorded in Bruker model using DMSO and  $\text{CDCl}_3$  as solvents. The observed peaks were correlated in ppm scale using tetra methyl silane as internal reference.

#### **2.2.3.3 Differential scanning calorimetry (DSC)**

The response of polymer towards heating can be investigated with the help of Differential scanning calorimetry (DSC) which follows basic heat flow technique and determines the corresponding transition points on comparing the heat supplied between the test and reference samples. This resulting difference depends on the composition as well as physical changes such as phase changes. From these transitions, glass transition temperature ( $T_g$ ) where a material takes the soft rubbery nature from hard brittle state can be obtained. The difference in heat output of the two heaters is recorded as a plot of heat (q) versus temperature (T).

The thermal properties of present linear polymers were evaluated on Perkin-Elmer DSC-7-instrument. Scans were run in nitrogen atmosphere at a heating rate of 10°C/min by placing minimum amount of sample in aluminium pan.  $T_g$  values were identified as the change in endothermic baseline.

#### 2.2.3.4 Thermo gravimetric analysis (TGA)

The thermal stability of a material can be analysed using thermo gravimetric analysis which also predicts the fraction of volatile components decomposed with the aid of weight loss occurring when a material is heated to a specific rate. Under inert atmosphere of nitrogen, measurement was carried out by recording the weight loss (%) with response to temperature. This technique provides different thermal data like  $T_{onset}$  (temperature where degradation begins),  $T_{max}$  (maximum degradation temperature), ash content ( $M_{res}$ ) commonly referred as char yield which forms a platform to evaluate its stability.

For the present set of thermal analysis, Perkin Elmer (TGS-2 model) thermal analyser was used to get a detailed insight on the thermal stability of the polymers and weight change undergone at temperature range upto 700°C at a heating rate of 20°C / min.

### 2.3 RESULTS AND DISCUSSION

The two series of polyesters synthesised by a facile polycondensation and interfacial polycondensation were characterised using appropriate techniques and presented below.

#### 2.3.1 Fourier transform Infra- red spectroscopy (FT-IR)

##### (i) Aliphatic polyesters

Polyesters of the present series varies only in the number of intervening methylene groups, whereas the remaining polymeric back bone seems to be identical. From **Figs. 2.1(a-h)**, various bands corresponding to the functional groups can be elicited. The characteristic band observed at a range of 3000  $\text{cm}^{-1}$ -3650  $\text{cm}^{-1}$  corresponds to the -OH stretching of glycerol hydroxyl groups. The presence of an ester functional group was confirmed by observing  $>\text{C}=\text{O}$  stretching bands of the carbonyl group around 1690  $\text{cm}^{-1}$ -1720  $\text{cm}^{-1}$  and  $>\text{C}-\text{O}-\text{C}<$  stretching of ether groups at a range of 1300  $\text{cm}^{-1}$ -1150  $\text{cm}^{-1}$ . The absence of aromatic nature was confirmed by the absence of  $>\text{C}=\text{C}<$  peaks in and around 1600  $\text{cm}^{-1}$ -1450  $\text{cm}^{-1}$ . **Table 2.3** summarizes the spectral data corresponding to various functional linkages present in the aliphatic polyesters.

##### (ii) Aromatic (cardo) polyesters

The FT-IR spectra of cardo polyesters predicted characteristic strong absorption bands in the region around 1690  $\text{cm}^{-1}$ -1730  $\text{cm}^{-1}$  and 1210  $\text{cm}^{-1}$ -1230  $\text{cm}^{-1}$  owing to the presence of  $>\text{C}=\text{O}$  and  $>\text{C}-\text{O}-\text{C}<$  stretching thereby confirming the ester functional groups as displayed in

**Figs. 2.2(a-h).** The absence of bands in the range of  $3000\text{ cm}^{-1}$ - $3600\text{ cm}^{-1}$  confirms the complete involvement of hydroxyl groups of monomer in polymerisation. However fine bands observed in this region might be due to the free end  $-\text{OH}$  groups. The stretching frequency of intervening methylene groups were observed in an appropriate range of  $2910\text{ cm}^{-1}$ - $2930\text{ cm}^{-1}$ . The characteristic absorption bands corresponding to  $>\text{C}=\text{C}<$  stretching of aromatic ring was predicted around  $1450\text{-}1600\text{ cm}^{-1}$ . The detailed spectral description of cardo polyesters are revealed in **Table 2.4**.

### 2.3.2 $^1\text{H}$ and $^{13}\text{C}$ Nuclear magnetic resonance spectroscopy

**$^1\text{H}$  NMR ( $\delta$ , ppm):** **Figs. 2.3(a-h)** and **Figs. 2.4(a-h)** corresponds to the  $^1\text{H}$  NMR spectra of aliphatic and aromatic (cardo) polyesters. The NMR spectra of aliphatic and aromatic polyesters were recorded using DMSO solvent whereas PGAZ (aliphatic) and MPOD (aromatic) were recorded under  $\text{CDCl}_3$  solubilised medium. Concerned with aliphatic polyesters multiplets observed in the range of  $1.2 - 1.8$  ppm corresponded to the methylene units connected to carbon ( $-\text{C}-\text{CH}_2-\text{C}-$ ). The  $-\text{CH}_2$  units attached with carbonyl group were confirmed by the peaks observed around  $2.2\text{-}2.4$  ppm. Methylene units attached with the electronegative atoms ( $-\text{O}-\text{CH}_2-\text{O}-$ ) were observed at  $3.9\text{-}4.1$  ppm (down field region) as multiplets followed by quintet at  $3.6\text{-}3.7$  ppm due to the methyne protons ( $-\text{CH}-$ ). The  $-\text{OH}$  protons appeared in the region around  $4.5\text{-}5$  ppm. In case of aromatic polyesters (**Figs. 2.4(a-h)**),  $-\text{CH}_2$  units of cyclohexane moiety were observed as multiplets below  $2$  ppm. Aliphatic spacers ( $-\text{CH}_2$  protons) were predicted around  $2.2\text{-}2.9$  ppm followed by aromatic protons above  $6.5$  ppm. Increased number of peaks and enlargement were observed in  $^1\text{H}$ -NMR spectrum, which could be reasoned due to the presence of repeated monomer in the resulting polymers under different environment<sup>47</sup>.

**$^{13}\text{C}$  NMR ( $\delta$ , ppm):** **Figs. 2.5(a-h)** and **Figs. 2.6(a-h)** elucidates the  $^{13}\text{C}$  NMR spectra of aliphatic and aromatic polyesters. Aliphatic polyesters (**Figs. 2.5(a-h)**) shows the carbonyl carbon ( $>\text{C}=\text{O}$ ) peaks around  $170$  ppm followed by the peaks of carbon connected to heteroatoms in the range of  $50\text{-}75$  ppm. The  $-\text{C}-\text{C}-$  peaks were observed in the range of  $20\text{-}35$  ppm. Aromatic polyesters (**Figs. 2.6(a-h)**) were associated with  $-\text{CH}_2-$  aliphatic carbons of cyclohexane moieties at a range of  $25\text{-}45$  ppm followed by alkyl spacer carbons at a range of  $23\text{-}35$  ppm. The aromatic carbons were found within  $120\text{-}150$  ppm whereas at a range of  $170$  ppm ester carbonyl carbons were found.

### 2.3.3 Differential scanning calorimetry (DSC)

The thermal events of the sample could be revealed by heating the material at a controlled rate of 10°C. As a function of temperature, DSC thermograms recorded for aliphatic and aromatic polyesters are displayed in **Fig. 2.7** and **Fig. 2.8**. From the plots, endothermic thermal events could be observed at a temperature range of 20°C to 350°C.

The data represented in **Table 2.5-2.6** pertains to the thermal properties of polyesters belonging to aliphatic and aromatic series. A DSC plot is generally accompanied with an endothermic change ( $T_g$ ) followed by the exothermic cold crystallisation ( $T_c$ ) and endothermic peak due to melting ( $T_m$ ). It is noteworthy that the glass transition ( $T_g$ ) does not occur suddenly at one unique temperature but rather at a range of temperature. The temperature in the middle of the inclined region is predicted as the  $T_g$ , the glass transition temperature.

It is precisely noted that above  $T_g$ , the polymer chains are accompanied with high mobility and enough energy to form ordered arrangements leading to crystalline nature with an exothermic peak which was followed by a melting temperature ( $T_m$ ) with an endothermic peak due to the enhanced mobility of polymeric chains creating disordered arrangement. It is not a criteria that all the polymers should experience  $T_g$ ,  $T_m$  and  $T_c$ .  $T_m$  and  $T_c$  were observed for the polymers that can form crystals while pure amorphous polymers experienced only  $T_g$ . From the plots it is evident that the materials were consistent to be amorphous, a non – crystalline nature due to the absence of successive peaks related to  $T_m$  and  $T_c$ . Increase in the length of alkyl chain of aliphatic polyesters enhances the  $T_g$  which could be subsequently due to its flexibility and associated molecular weight which decreases its chain end concentration in turn decreasing free volume at end group. Introduction of bulky cardo substituents in aromatic polyesters increases the  $T_g$  due to decreased mobility. The higher  $T_g$  values observed for cardo polyesters could be reasoned due to increased size of cardo moieties whose bulky non-coplanar structure cannot orient themselves into a definite direction and consequently cannot move in to the closer proximities of molecular chains<sup>48</sup>. Moreover cardo group generally increases the chain rigidity restricting the free rotation of polymer back bone resulting with higher  $T_g$  compared with aliphatic polyesters<sup>49</sup>.

#### **2.3.4 Thermogravimetric analysis (TGA)**

Thermogravimetric analysis is a technique utilised to study the mass change due to the decomposition or redox reactions occurring as a function of temperature. Each TG curve will be accompanied with procedural decomposition temperature [ $T_i$ ] where the onset mass change begins and [ $T_f$ ] the final temperature where the process gets completed. The difference of [ $T_f - T_i$ ] does not possess any fixed values rather it depends on the experimental conditions.

**Figs. 2.9-2.10** represents the TGA curves of aliphatic and aromatic polyesters with its corresponding data in **Table 2.5-2.6**.

Close observation of the figures and data revealed that the aliphatic polyesters were stable in the range of 190°C - 305°C whereas cardo polyesters were within 230°C - 429°C with a char residue of less than 5%. All the observed  $T_{\max}$  values showed close proximity suggesting the similar decomposition mechanism. The major degradation of polyesters (PGM, PGS, PGG, PGA, PGP, PGSU, PGAZ, PGSE) takes place due to the scission of polymer main chain whereas in cardo polyesters it was predominantly due to the cleavage of bulky cyclohexane moiety. In general, aromatic system has greater thermal stability than aliphatic polymers<sup>50</sup>. The TGA curves of all the aromatic polyesters shows small weight loss below 100°C which may be due to the loss of moisture and entrapped solvents. Increase in length of alkyl moieties increases the thermal stability<sup>51</sup>. The main degradation mechanism of polyesters endeavours the formation of alkenes, through  $\beta$ -elimination, trans-esterification and the rearrangements involving the end-groups playing a decisive role on the thermal stability of polyesters. But in the present discussion, concerned with aromatic polyesters introduction of cyclohexane moiety hampers the polymer packing thereby stiffening the back bone of polymer leading to chain separation and decreasing strong intermolecular interactions<sup>52</sup>.

## 2.4 CONCLUSIONS

The following conclusions can be retrieved from the above discussions

- (i) A series of aliphatic and aromatic (cardo) polyesters were synthesised.
- (ii) Structure of the synthesised polyesters were confirmed by FT-IR and NMR spectral analysis.
- (iii) Thermal response of the synthesised polyesters were studied using TGA and DSC analysis where aromatic polyesters possessed higher  $T_g$  and thermal stability than aliphatic polyesters.



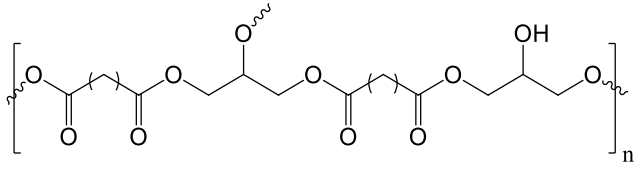
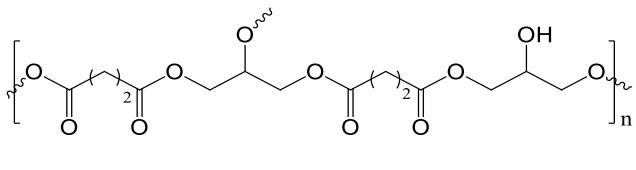
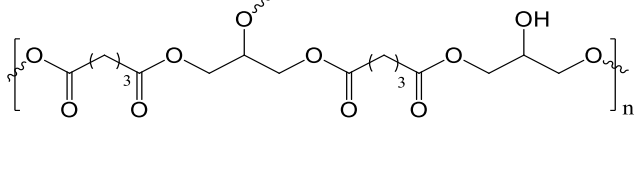
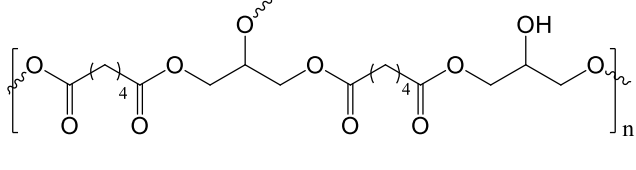
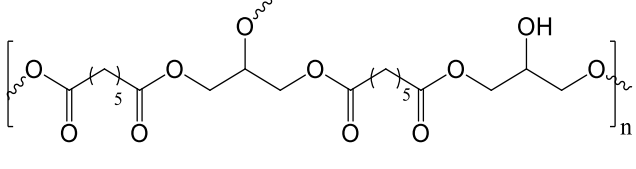
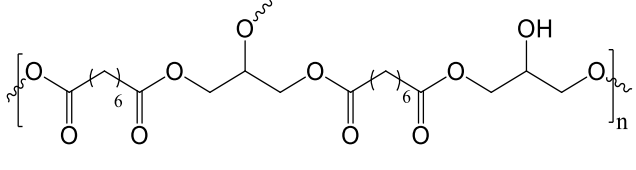
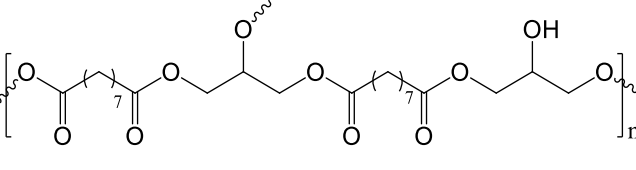
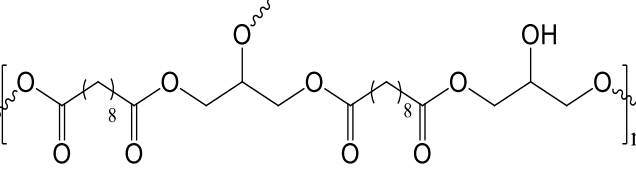
## 2.5 REFERENCES

1. J. Scheirs, T.E. Long, *Modern polyesters: chemistry and technology of polyesters and copolyesters*, John Wiley & Sons, Hoboken, NJ, (2003).
2. A.C. Albertsson, I. Varma, *Adv. Polym. Sci.*, **157** (2002) 1-40.
3. A.C. Albertsson, I.K. Varma, *Biomacromolecules.*, **4(6)** (2003) 1466-1486.
4. R. Jain, *Drug Dev. Ind. Pharm.*, **24(8)** (1998) 703-727.
5. J. Kasperczyk, *Polym. Degrad. Stabil.*, **93(5)** (2008) 990-999.
6. M. Vert, *J. Control. Release.*, **53(1-3)** (1998) 85-92.
7. R.J. Müller, *Handbook of Biodegradable Polymers*, Rapra Technology: Shawbury, (2005).
8. J.L. Liu, L. Wang, Z. Zhen, X.H. Liu, *Colloid Polym. Sci.*, **290** (2012) 1215–1220.
9. G. Zhang, X.J. Xing, D.S. Li, X.J. Wang, J. Yang, *Ind. Eng. Chem. Res.*, **52** (2013) 16577–16584.
10. K.A. Ellzey, T. Ranganathan, J. Zilberman, E.B. Coughlin, R.J. Farris, T. Emrick, *Macromol.*, **39** (2006) 3553–3558.
11. G.S. Liou, S.H. Hsiao, H.M. Huang, C.W. Chang, H.J. Yen, *J. Polym. Res.*, **14** (2007) 191–199.
12. R. Smith, *Biodegradable polymers for industrial applications*, Wood Head Publishing limited, (2005), First edition.
13. M. Gigli, M. Fabbri, N. Lotti, R. Gamberini, B. Rimini, A. Munari, *Eur. Polym. J.*, **75** (2016) 431-460.
14. V. Tsanaktsis, Z. Terzopoulou, M. Nerantzaki, G.Z. Papageorgiou, D.N. Bikiaris, *Mater. Lett.*, **178** (2016) 64-67.
15. X. Ma, H. Niu, W. Cai, T. Xiao, C. Wang, *React. Funct. Polym.*, **108** (2016) 63-70.
16. B. Nottelet, V. Darcos, J. Coudane, *Eur. J. Pharm. Biopharm.*, **97** (2015) 350-370.
17. A.C. Fonseca, I.M. Lopes, J.F.J. Coelho, A.C. Serra, *React. Funct. Polym.*, **97** (2015) 1-11.
18. J.N. Korley, S. Yazdi, K. McHugh, J. Kirk, J. Anderson, D. Putnam, *Biomaterials.*, **8** (2016) 41-52.
19. G.Z. Papageorgiou, N. Guigo, V. Tsanaktsis, D.G. Papageorgiou, S. Exarhopoulos, N. Sbirrazzuoli, D.N. Bikiaris, *Eur. Polym. J.*, **68** (2015) 115-127.
20. G. Totaro, L. Cruciani, M. Vannini, G. Mazzola, D.D. Gioia, A. Celli, L. Sisti, *Eur. Polym. J.*, **56** (2014) 174-184.

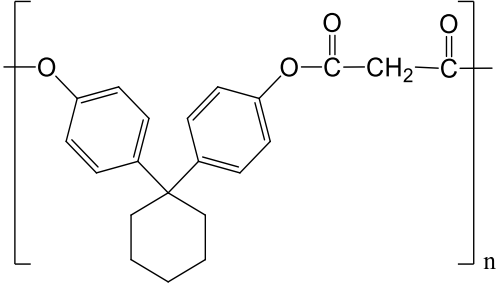
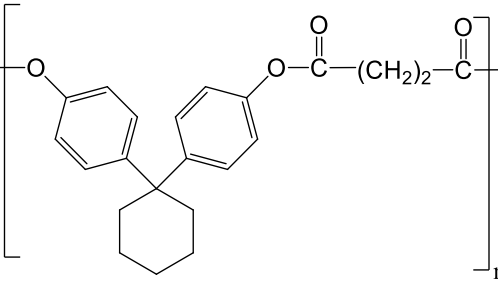
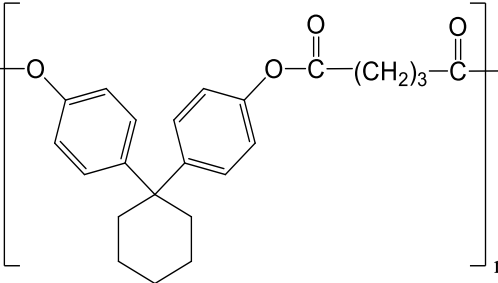
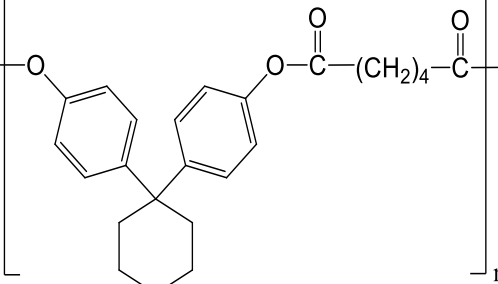
21. A. Tanaka, M. Kohri, T. Takiguchi, M. Kato, S. Matsumura, *Polym. Degrad. Stabil.*, **97(8)** (2012) 1415-1422.
22. A. Noreen, K.M. Zia, M. Zuber, M. Ali, M. Mujahid, *Int. J. Biol. Macromol.*, **86** (2016) 937-949.
23. D.H. Guimaraesa, B. Michel de Meireles, F. Raigens da Paz, L.A. Sanches de Almeida Pradob, J.S. Boaventuraa, N.M. Josea, *Mater. Res.*, **10(3)** (2007) 257-260.
24. G.S.P. Littis Malar, S.B. David, *Int. J. Sci. Res.*, **4(2)** (2015) 1960-1964.
25. M.S. Mohammadnia, P. Salaryan, Z.K. Azimi, F.T. Seyidov, *Int. J. Chem. Biochem. Res.*, **2** (2012) 36-41.
26. B.J. Vasanthi, L. Ravikumar, *J. Polym. Chem.*, **3** (2013) 70-77.
27. A. Diaz, R. Katsarava, J. Puiggali, *Int. J. Mol. Sci.*, **15** (2014) 7064-7123.
28. R. Indira, T. Tamizharuvi, T.V. Rajendran, V. Jaisankar, *Indian. J. Adv. Chem. Sci.*, **1(4)** (2013) 250-255.
29. L. Cabrales, K. Calderon, I. Hinojosa, F. Valencia, N. Abidi, *Int. J. Polym. Anal. Charact.*, **21(8)** (2016) 718-727.
30. N. Li, F. Zeng, D. Qu, J. Zhang, L. Shao, Y. Bai, *J. Appl. Polym. Sci.*, **133(46)** (2016) 1-11.
31. J.M. Dennis, J.S. Enokida, T.E. Long, *Macromol.*, **48(24)** (2015) 8733-8737.
32. J. Wu, P. Eduard, L. Jasinska-Walc, A. Rozanski, B.A.J. Noordover, D.S. van Es, C.E. Koning, *Macromol.*, **46(2)** (2013) 384-394.
33. T.J. Farmer, R.L. Castle, J.H. Clark, D.J. Macquarrie, *Int. J. Mol. Sci.*, **16(7)** (2015) 14912-14932.
34. D. Senol, I. Kaya, *J. Saudi. Chem. Soc.*, **21(5)** (2017) 505-516.
35. B. Abderrahim, E. Abderrahman, A. Mohamed, A. Aicha, B. Reda, A. Abdeslam, J. Isaad, T. Abdesselam, *J. Polym. Biopolymer. Phys. Chem.*, **4(1)** (2016) 16-27.
36. A.V. Kavimani, B.V. Jaisankar, *Indian. J. Adv. Chem. Sci.*, **3(2)** (2015) 192-197.
37. G.S.P. Littis Malar, S.B. David, *Int. J. Sci. Eng. Appl. Sci.*, **1(5)** (2015) 142-148.
38. M.H. Bilal, M. Prehm, A.E. Njau, M.H. Samiullah, A. Meister, J. Kressler, *Polym.*, **8(3)** (2016) 1-11.
39. A.C. Albertsson, I. Varma, *Adv. Polym. Sci.*, **157** (2002) 1-40.
40. X. Lou, C. Detrembleur, Ph. Lecomte, R. Jerome, *Macromol.*, **34(17)** (2001) 5806-5811.

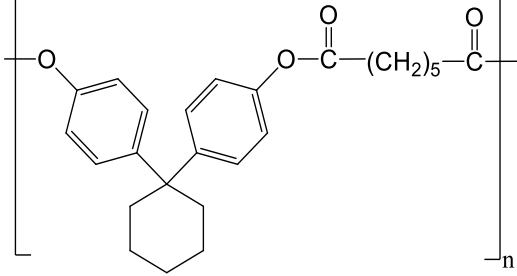
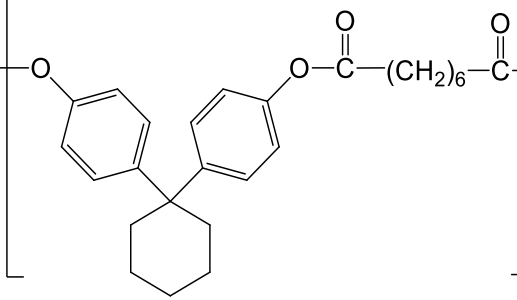
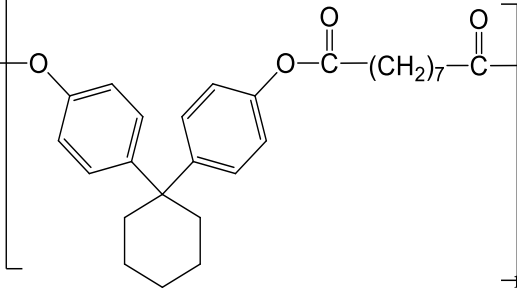
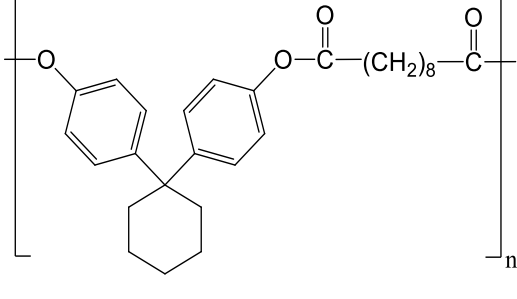
41. S. Kobayashi, H. Uyama, S. Kimura, *Chem. Rev.*, **101(12)** (2001) 3793-3818.
42. T. Chongcharoenchaikul, P. Thamyongkit, S. Poompradub, *Mater. Chem. Phys.*, **177** (2016) 485-495.
43. S.G. Sanadhya, S.L. Oswal, K.C. Parmar, *J. Chem. Pharm. Res.*, **6(4)** (2014) 705-714.
44. J.A. Moore, J.E. Kelly, *Polym.*, **20(5)** (1979) 627-628.
45. P.N. Honkhambe, N.S. Bhairamadgi, M.V. Biyani, P.P. Wadgaonkar, M.M. Salunkhe, *Eur. Polym. J.*, **46** (2010) 709–718.
46. S.G. Sanadhya, S.L. Oswal, K.C. Parmar, *Der Pharm. Chemica.*, **6(6)** (2014) 156-163.
47. D. Senol, I. Kaya, *J. Saudi. Chem. Soc.*, **21(5)** (2017) 505-516.
48. S.S. Vibhute, M.D. Joshi, P.P. Wadgaonkar, A.S. Patil, N.N. Maldar, *J. Polym. Sci., Part A : Polym. Chem.*, **35** (1997) 3227-3234.
49. L. Der-Jang, H. Jun-Jang, L. Been-Yang, *J. Polym. Sci., Part A : Polym. Chem.*, **39** (2001) 2951-2956.
50. B.A. Sweileh, Y.M. Al-Hiari, M.H. Kailani, H.A. Mohammad, *Molecules.*, **15** (2010) 3661-3682.
51. E. Zakharova, A. Martínez de Ilarduya, S. Leon, S.M. Guerra, *Des. Monomers Polym.*, **20(1)** (2017) 157-166.
52. G. Latha, M. Natarajan, K. Balaji, S. C. Murugavel, *High Perform. Polym.*, **26(2)** (2014) 125–134.

**Table 2.1 Structure of aliphatic polyesters**

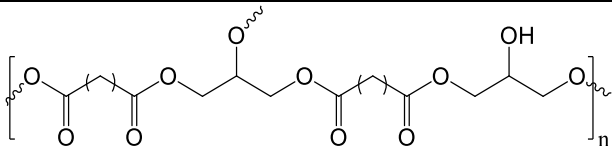
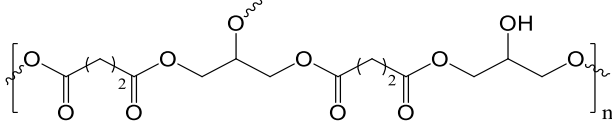
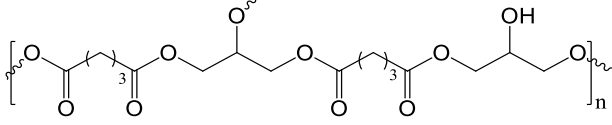
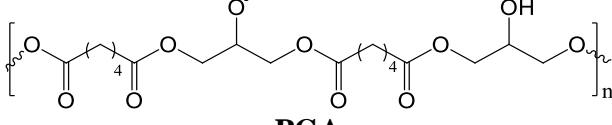
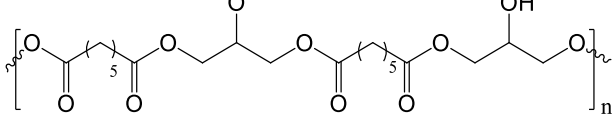
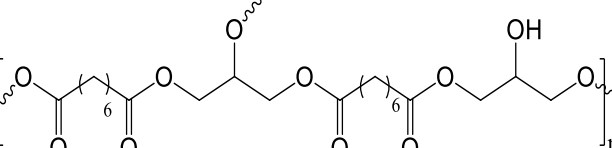
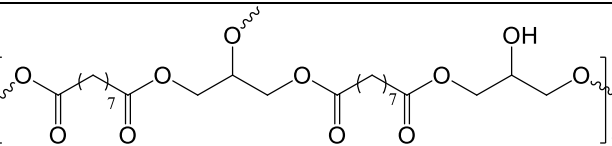
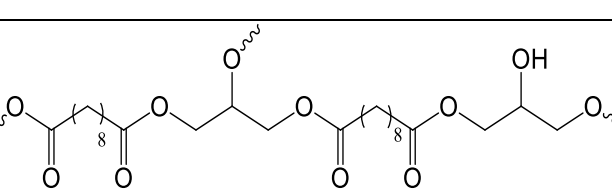
Name of the polyester	Structure of the polyester
Poly (glycerol malonate) <b>(PGM)</b>	
Poly (glycerol succinate) <b>(PGS)</b>	
Poly (glycerol glutarate) <b>(PGG)</b>	
Poly (glycerol adipate) <b>(PGA)</b>	
Poly (glycerol pimelate) <b>(PGP)</b>	
Poly (glycerol suberate) <b>(PGSU)</b>	
Poly (glycerol azelate) <b>(PGAZ)</b>	
Poly (glycerol sebacate) <b>(PGSE)</b>	

**Table 2.2 Structure of aromatic (cardo) polyesters**

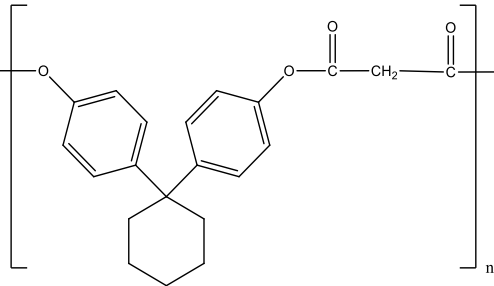
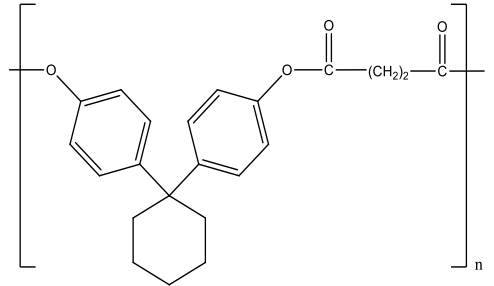
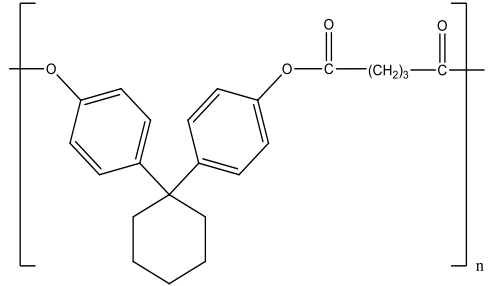
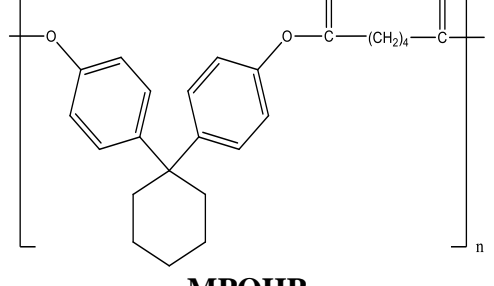
Name of the polyester	Structure of the polyester
<p>4-(1-(4-methoxyphenyl)cyclohexyl) phenyl 3-oxobutanoate <b>(MPOB)</b></p>	 <p>The structure shows a central cyclohexane ring substituted with two 4-methoxyphenyl groups. One of these phenyl groups is linked via an oxygen atom to the carbonyl group of a 3-oxobutanoate chain. The entire unit is enclosed in brackets with a subscript 'n'.</p>
<p>4-(1-(4-methoxyphenyl)cyclohexyl) phenyl 4-oxopentanoate <b>(MPOP)</b></p>	 <p>The structure is similar to MPOB, but the aliphatic chain between the two carbonyl groups consists of two methylene groups, (CH<sub>2</sub>)<sub>2</sub>.</p>
<p>4-(1-(4-methoxyphenyl)cyclohexyl) phenyl 5-oxohexanoate <b>(MPOHX)</b></p>	 <p>The structure is similar to MPOB, but the aliphatic chain between the two carbonyl groups consists of three methylene groups, (CH<sub>2</sub>)<sub>3</sub>.</p>
<p>4-(1-(4-methoxyphenyl)cyclohexyl) phenyl 6-oxoheptanoate <b>(MPOHP)</b></p>	 <p>The structure is similar to MPOB, but the aliphatic chain between the two carbonyl groups consists of four methylene groups, (CH<sub>2</sub>)<sub>4</sub>.</p>

<p>4-(1-(4-methoxyphenyl)cyclohexyl) phenyl 7-oxooctanoate <b>(MPOO)</b></p>	
<p>4-(1-(4-methoxyphenyl)cyclohexyl) phenyl 8-oxononanoate <b>(MPON)</b></p>	
<p>4-(1-(4-methoxyphenyl)cyclohexyl) phenyl 9-oxodecanoate <b>(MPOD)</b></p>	
<p>4-(1-(4-methoxyphenyl)cyclohexyl) phenyl 10-oxoundecanoate <b>(MPOU)</b></p>	

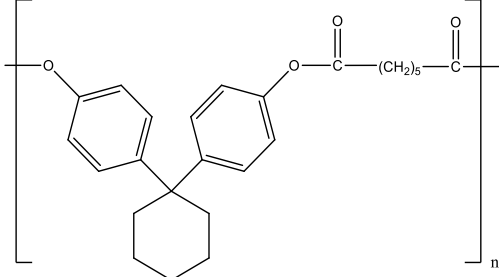
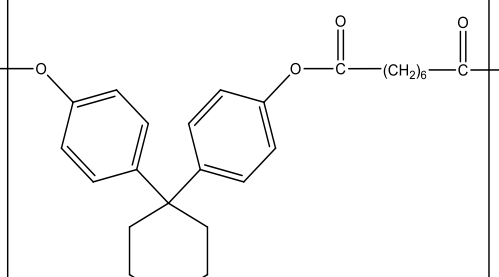
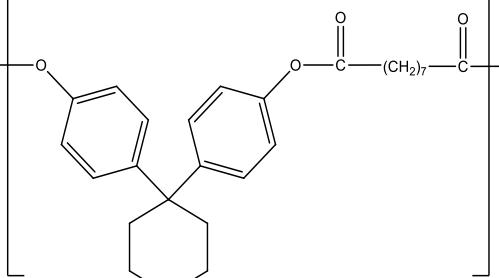
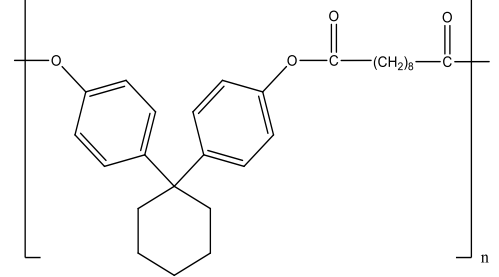
**Table 2.3 FT-IR spectral data of aliphatic polyesters**

Structure of the polyester	IR frequencies (cm <sup>-1</sup> )
 <p style="text-align: center;"><b>PGM</b></p>	$\nu$ -OH 3361.51 $\nu$ >C=O 1716.25 $\nu$ -C-O-C- 1240.41
 <p style="text-align: center;"><b>PGS</b></p>	$\nu$ -OH 3392.51 $\nu$ >C=O 1713.24 $\nu$ -C-O-C- 1163.23
 <p style="text-align: center;"><b>PGG</b></p>	$\nu$ -OH 3467.17 $\nu$ >C=O 1710.73 $\nu$ -C-O-C- 1147.01
 <p style="text-align: center;"><b>PGA</b></p>	$\nu$ -OH 3336.43 $\nu$ >C=O 1711.17 $\nu$ -C-O-C- 1159.6
 <p style="text-align: center;"><b>PGP</b></p>	$\nu$ -OH 3495.35 $\nu$ >C=O 1708.13 $\nu$ -C-O-C- 1178.19
 <p style="text-align: center;"><b>PGSU</b></p>	$\nu$ -OH 3335.24 $\nu$ >C=O 1692.38 $\nu$ -C-O-C- 1257.72
 <p style="text-align: center;"><b>PGAZ</b></p>	$\nu$ -OH 3303.24 $\nu$ >C=O 1701.29 $\nu$ -C-O-C- 1242.21
 <p style="text-align: center;"><b>PGSE</b></p>	$\nu$ -OH 3300 $\nu$ >C=O 1693.57 $\nu$ -C-O-C- 1296.22

**Table 2.4 FT-IR spectral data of aromatic (cardo) polyesters**

Structure of the polyester	IR frequencies (cm <sup>-1</sup> )
 <p style="text-align: center;"><b>MPOB</b></p>	$\nu >C=O$ 1733.83 $\nu -C-O-C-$ 1227.05 $\nu >C=C<$ 1630.07 $\nu -CH_2$ str 2919.39
 <p style="text-align: center;"><b>MPOP</b></p>	$\nu >C=O$ 1715.76 $\nu -C-O-C-$ 1221.96 $\nu >C=C<$ 1635.71 $\nu -CH_2$ str 2920.35
 <p style="text-align: center;"><b>MPOHX</b></p>	$\nu >C=O$ 1707.08 $\nu -C-O-C-$ 1216.17 $\nu >C=C<$ 1641.49 $\nu -CH_2$ str 2920.35
 <p style="text-align: center;"><b>MPOHP</b></p>	$\nu >C=O$ 1713.83 $\nu -C-O-C-$ 1229.67 $\nu >C=C<$ 1628.95 $\nu -CH_2$ str 2920.35



 <p style="text-align: center;"><b>MPOO</b></p>	$\nu >C=O$ 1727.33 $\nu -C-O-C-$ 1217.14 $\nu >C=C<$ 1512.26 $\nu -CH_2 \text{ str}$ 2927.10
 <p style="text-align: center;"><b>MPON</b></p>	$\nu >C=O$ 1696.47 $\nu -C-O-C-$ 1231.60 $\nu >C=C<$ 1416.78 $\nu -CH_2 \text{ str}$ 2923.25
 <p style="text-align: center;"><b>MPOD</b></p>	$\nu >C=O$ 1710.93 $\nu -C-O-C-$ 1228.71 $\nu >C=C<$ 1589.41 $\nu -CH_2 \text{ str}$ 2919.39
 <p style="text-align: center;"><b>MPOU</b></p>	$\nu >C=O$ 1719.61 $\nu -C-O-C-$ 1224.85 $\nu >C=C<$ 1518.22 $\nu -CH_2 \text{ str}$ 2926.34

**Table 2.5 Thermal data from DSC and TGA thermograms of aliphatic polyesters**

<b>Name of the polyester</b>	<b>T<sub>g</sub> (°C)</b>	<b>T<sub>10</sub> (°C)</b>	<b>T<sub>max</sub> (°C)</b>	<b>Char yield (%)</b>
<b>PGM</b>	95	188.44	190.06	57.60
<b>PGS</b>	97	158.94	201.03	52.63
<b>PGG</b>	109	186.66	250.34	40.74
<b>PGA</b>	110	191.28	257.35	37.41
<b>PGP</b>	115	194.15	269.89	50.15
<b>PGSU</b>	117	181.14	251.41	35.98
<b>PGAZ</b>	120	210.11	286.41	56.39
<b>PGSE</b>	126	191.28	305.82	40.59

**Table 2.6 Thermal data from DSC and TGA thermograms of aromatic (cardo) polyesters**

<b>Name of the polyester</b>	<b>T<sub>g</sub> (°C)</b>	<b>T<sub>10</sub> (°C)</b>	<b>T<sub>max</sub> (°C)</b>	<b>Char yield (%)</b>
<b>MPOB</b>	130	81.60	230.68	0.44
<b>MPOP</b>	135	133.48	408.41	1.3
<b>MPOHX</b>	146	194.48	411.40	1.86
<b>MPOHP</b>	155	141.57	419.26	0.49
<b>MPOO</b>	185	179.43	421.07	4.2
<b>MPON</b>	200	124.83	423.03	3.6
<b>MPOD</b>	203	152.50	431.22	3.3
<b>MPOU</b>	280	188.92	429.56	3.17

### FT-IR Spectra of aliphatic polyesters

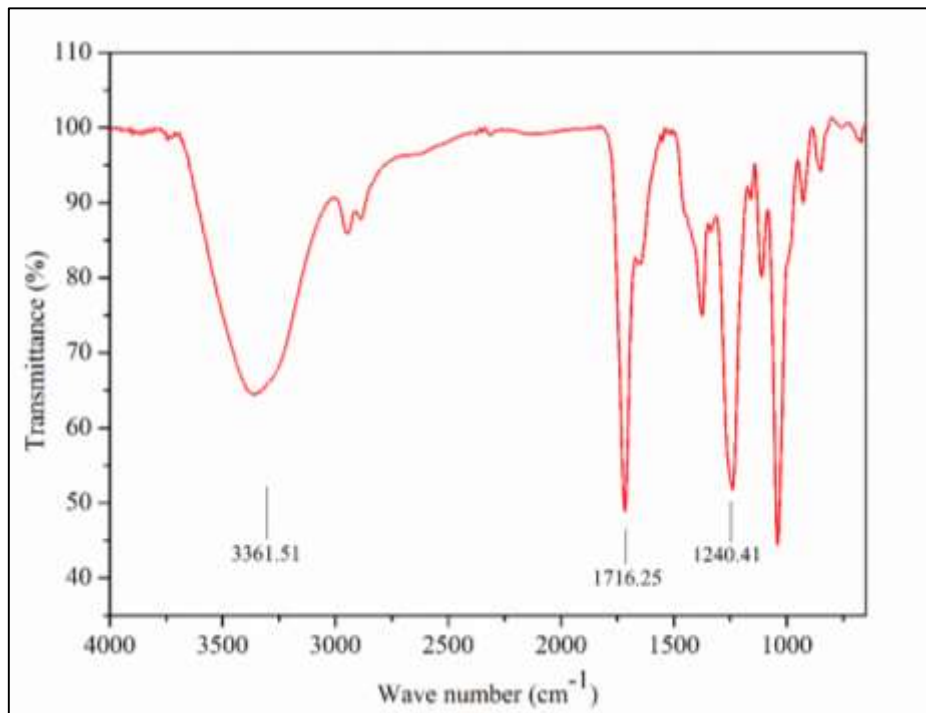


**Fig. 2.1(a) FT-IR spectrum of PGM**

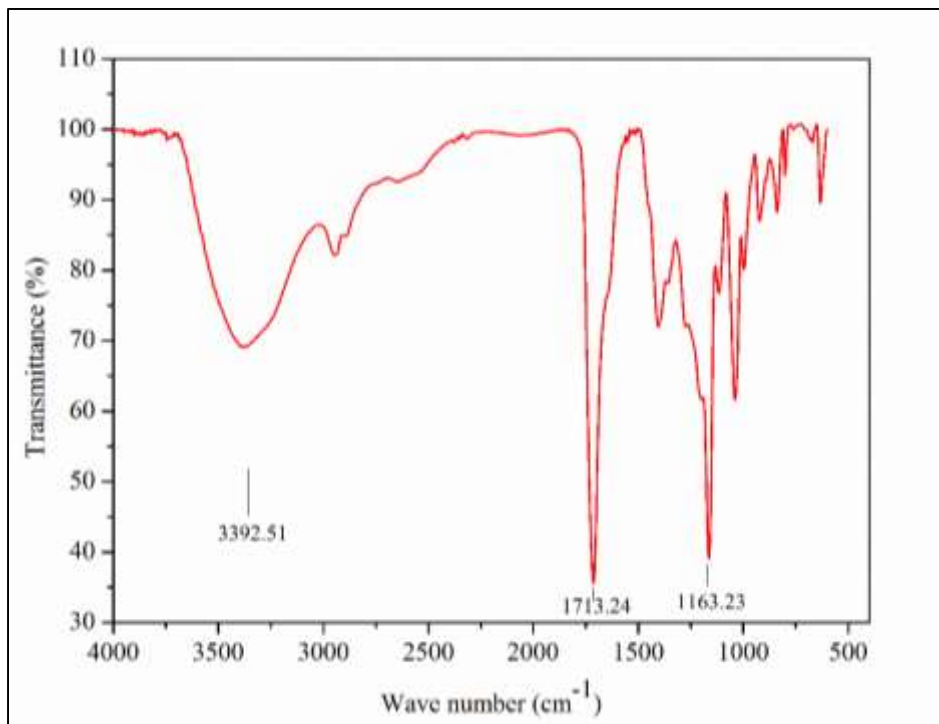


**Fig. 2.1(b) FT-IR spectrum of PGS**

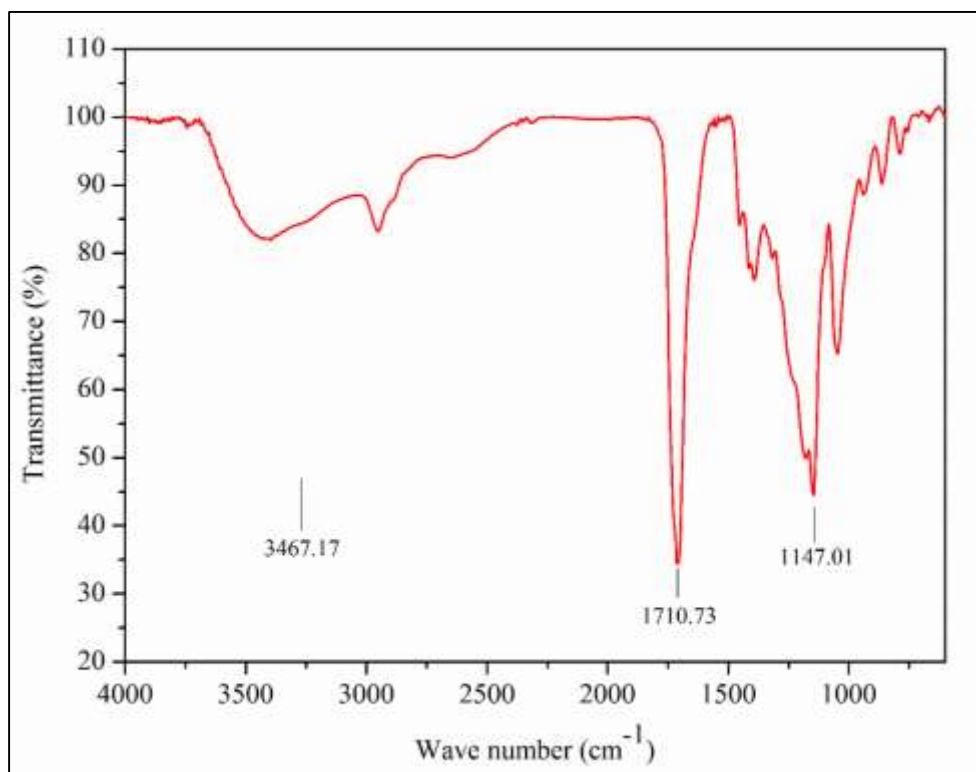


**Fig. 2.1(c) FT-IR spectrum of PGG**

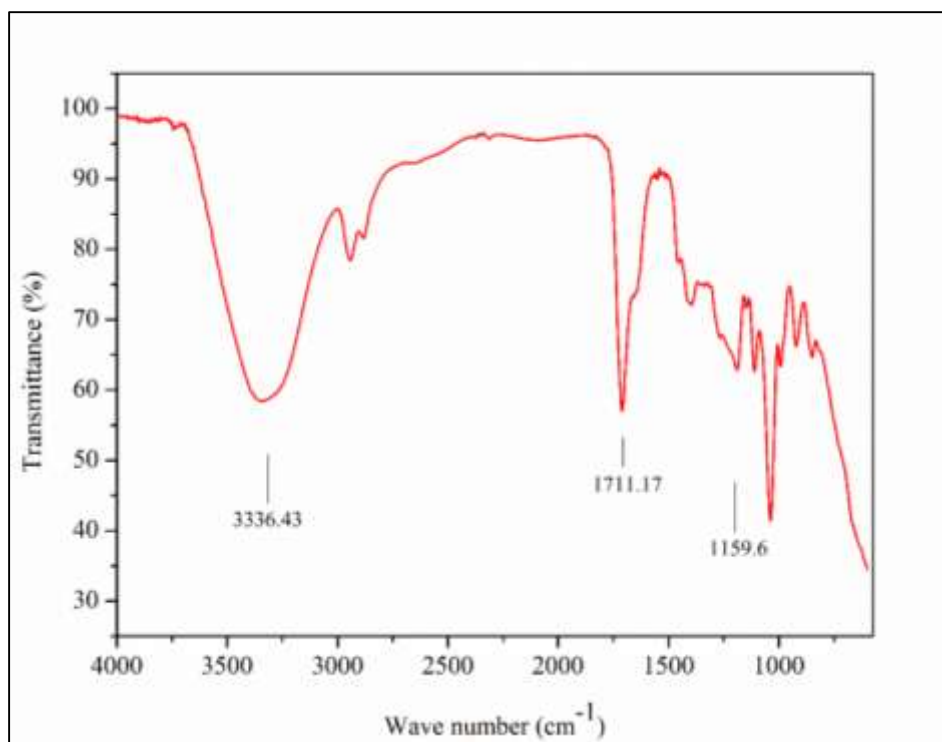


**Fig. 2.1(d) FT-IR spectrum of PGA**

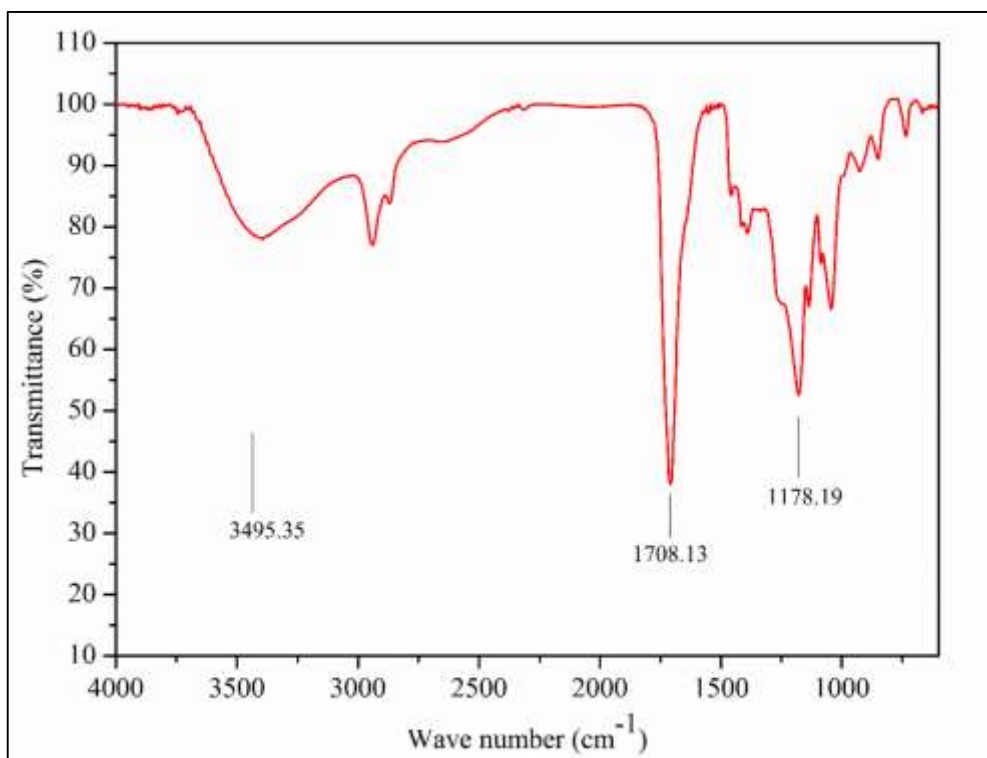


**Fig. 2.1(e) FT-IR spectrum of PGP**

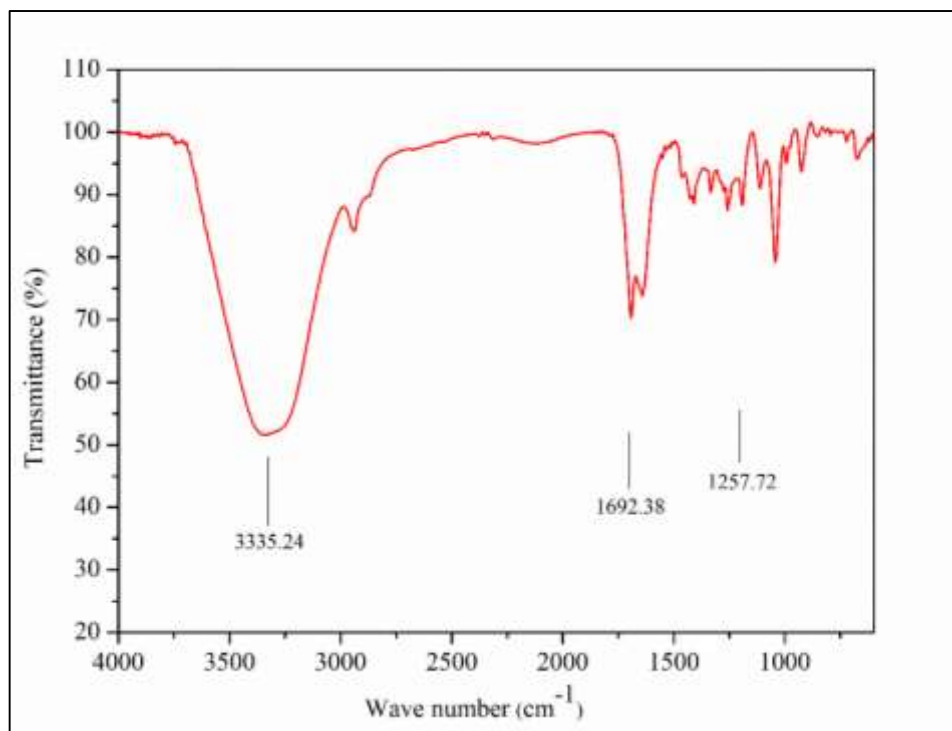


**Fig. 2.1(f) FT-IR spectrum of PGSU**

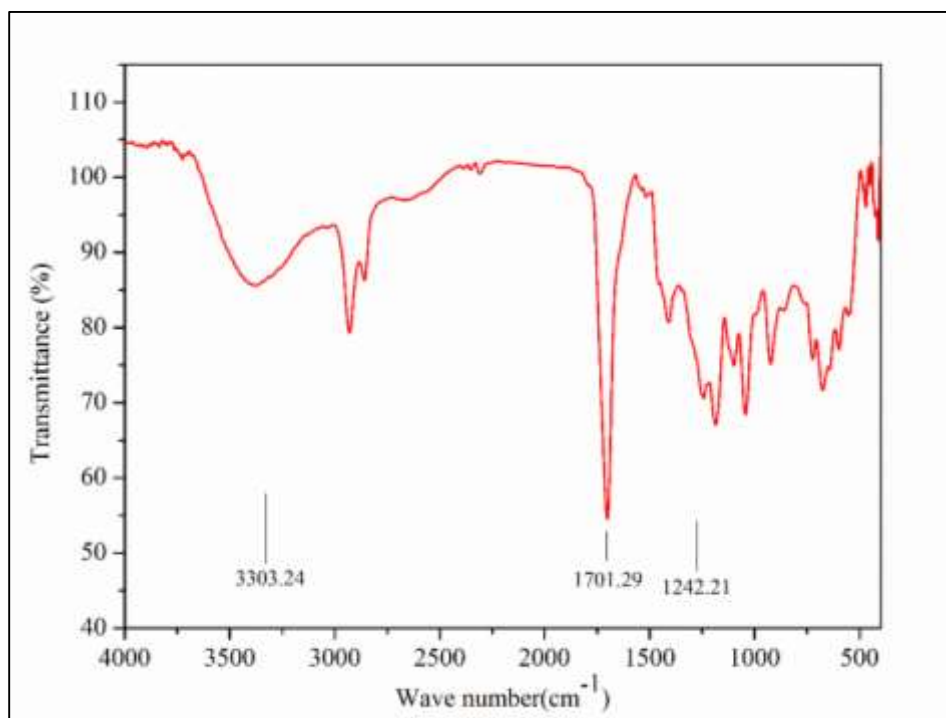


**Fig. 2.1(g) FT-IR spectrum of PGAZ**

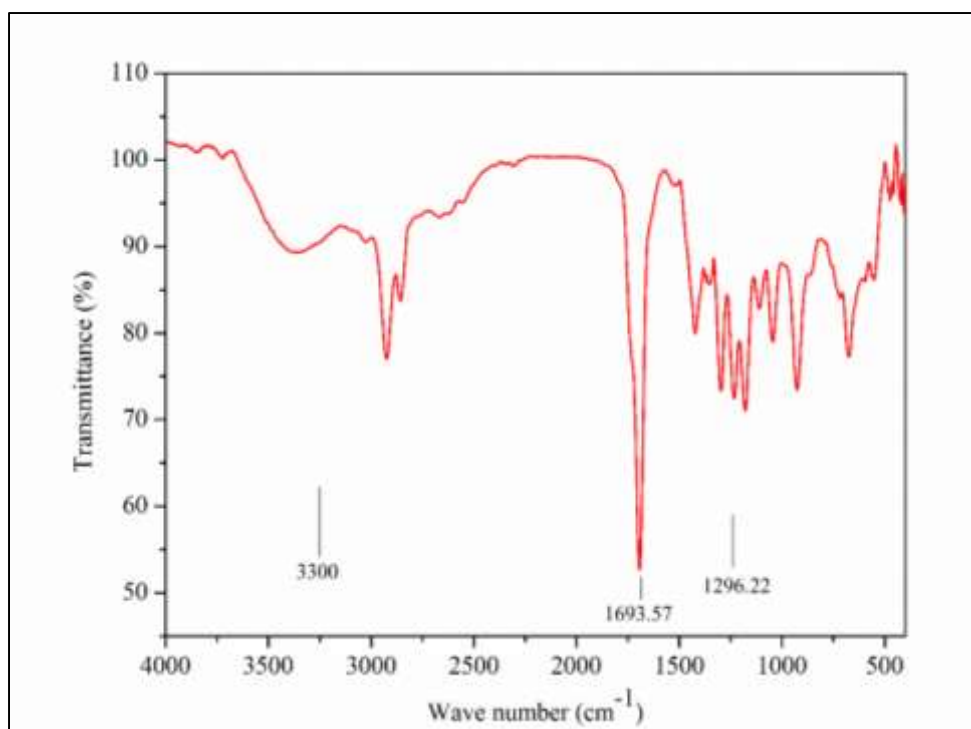


**Fig. 2.1(h) FT-IR spectrum of PGSE**

### FT-IR Spectra of aromatic (cardo) polyesters

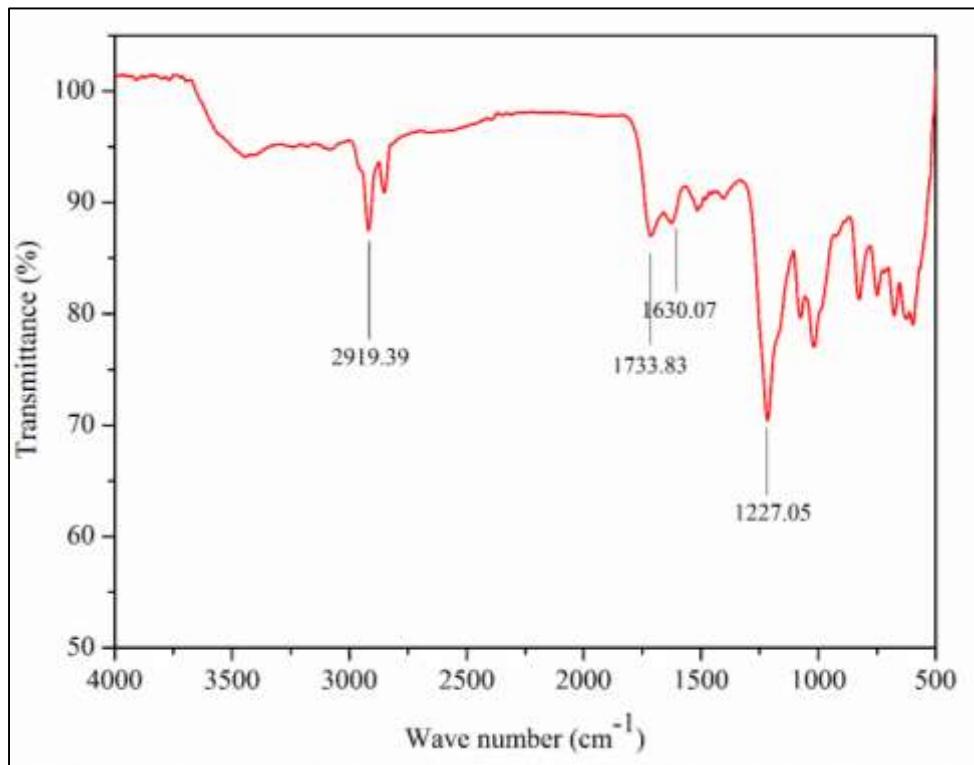


**Fig. 2.2(a) FT-IR spectrum of MPOB**

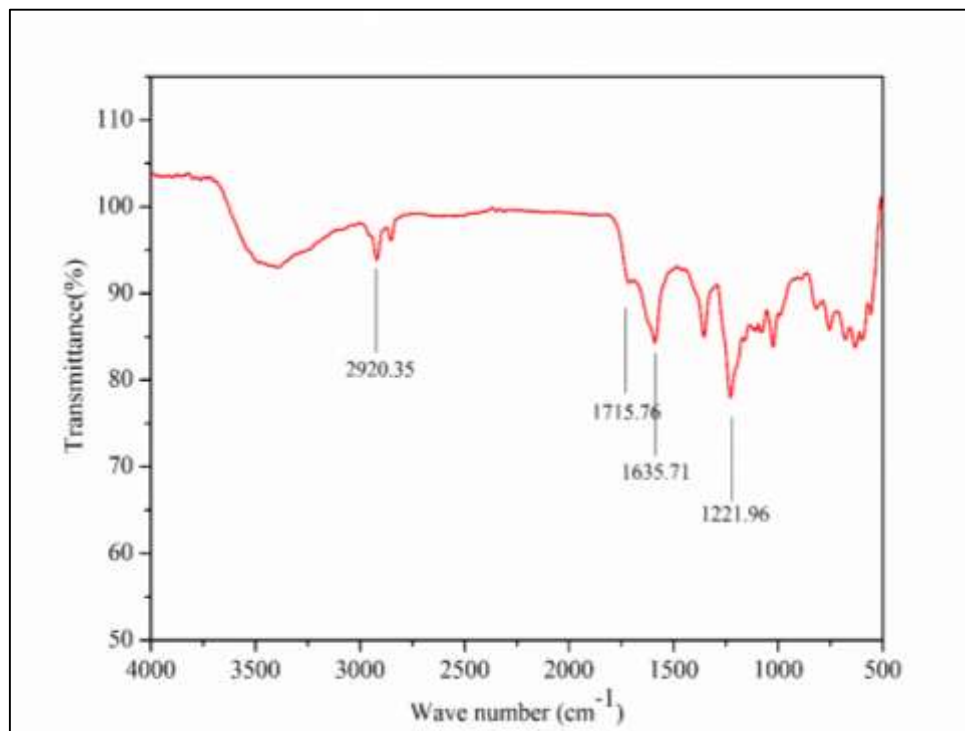


**Fig. 2.2(b) FT-IR spectrum of MPOP**

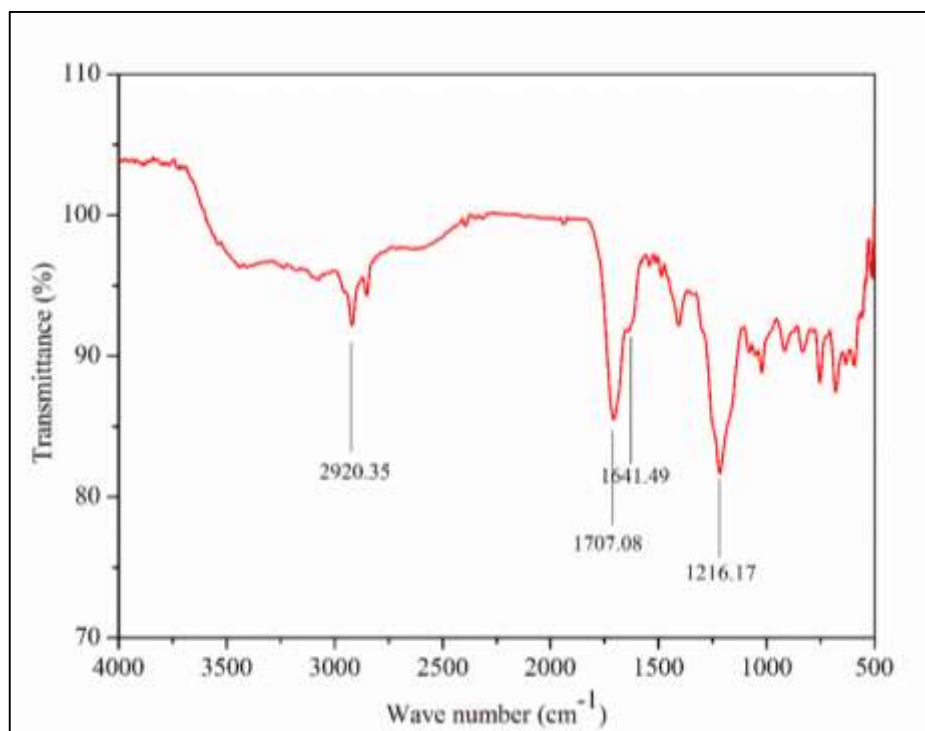


**Fig. 2.2(c) FT-IR spectrum of MPOHX**

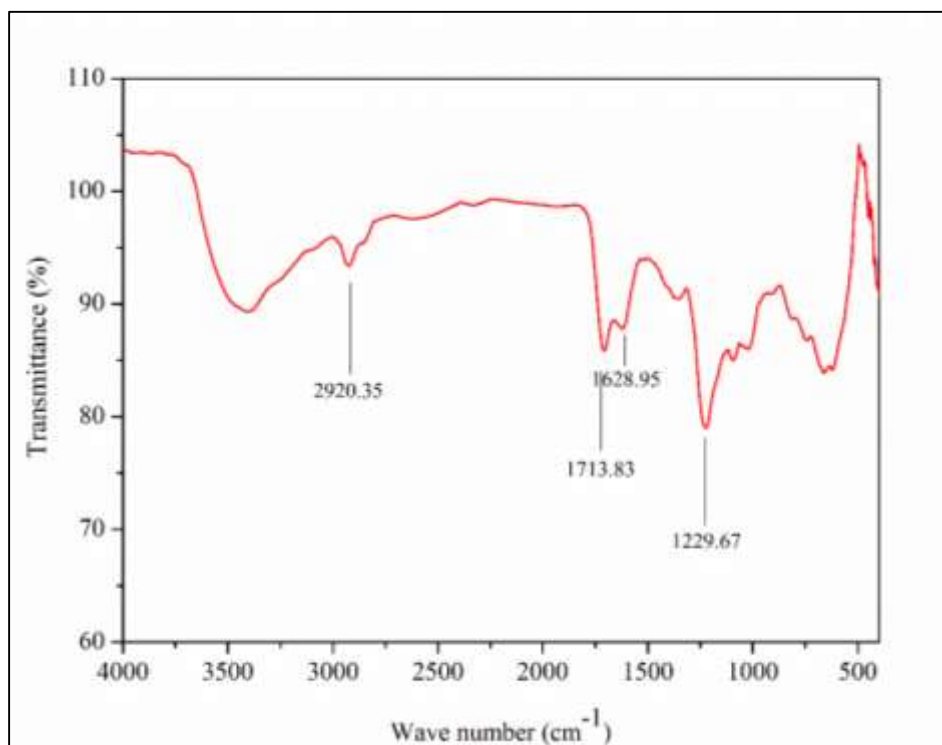


**Fig. 2.2(d) FT-IR spectrum of MPOHP**



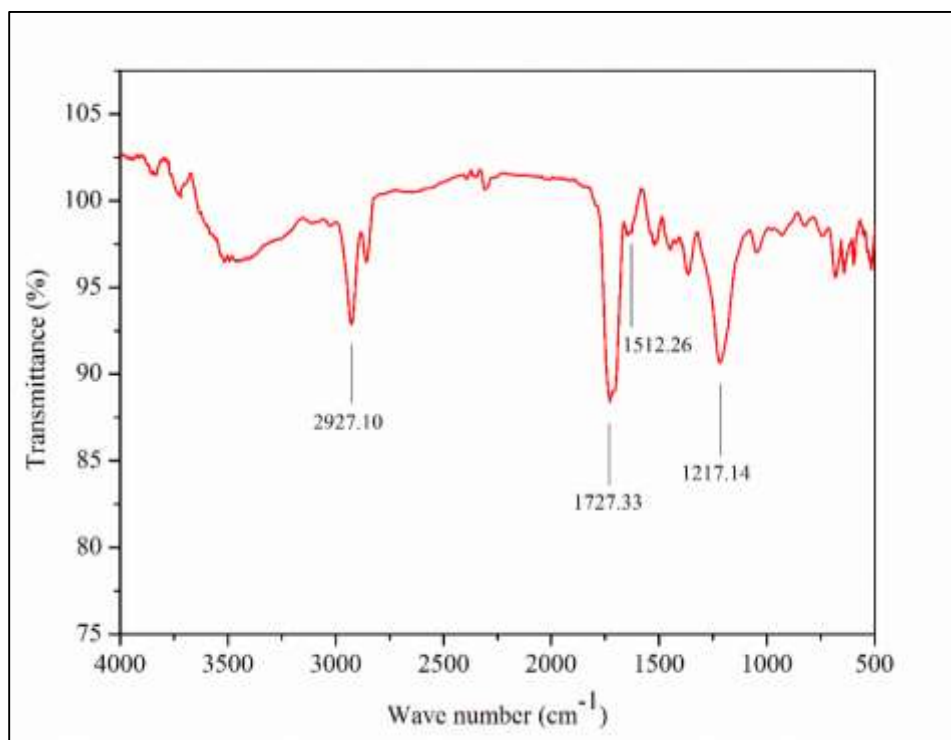


**Fig. 2.2(e) FT-IR spectrum of MPOO**

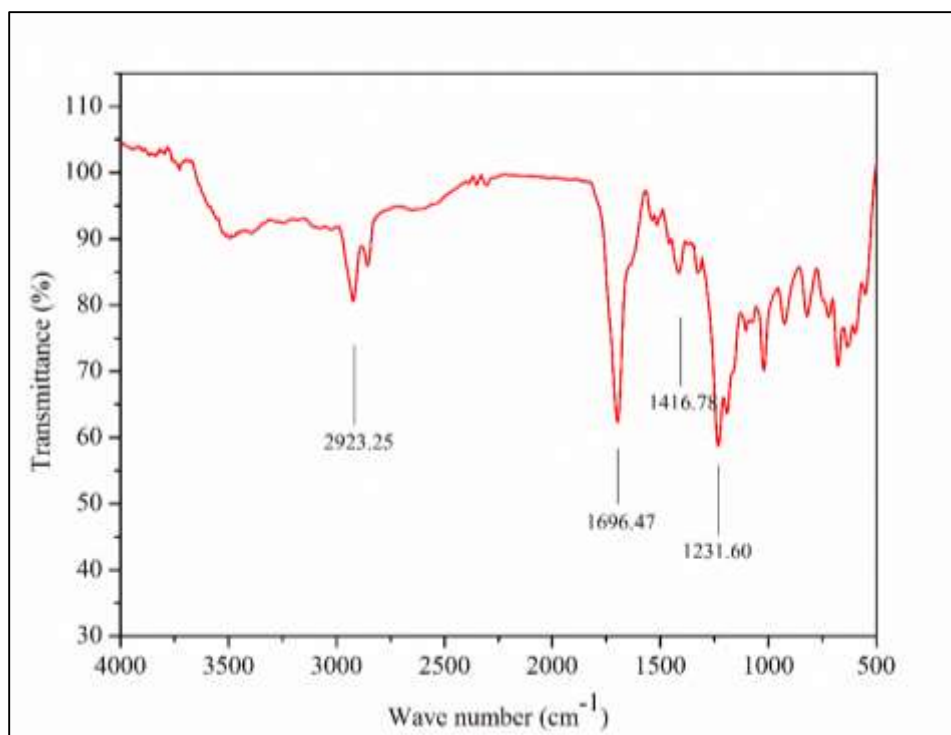


**Fig. 2.2(f) FT-IR spectrum of MPON**

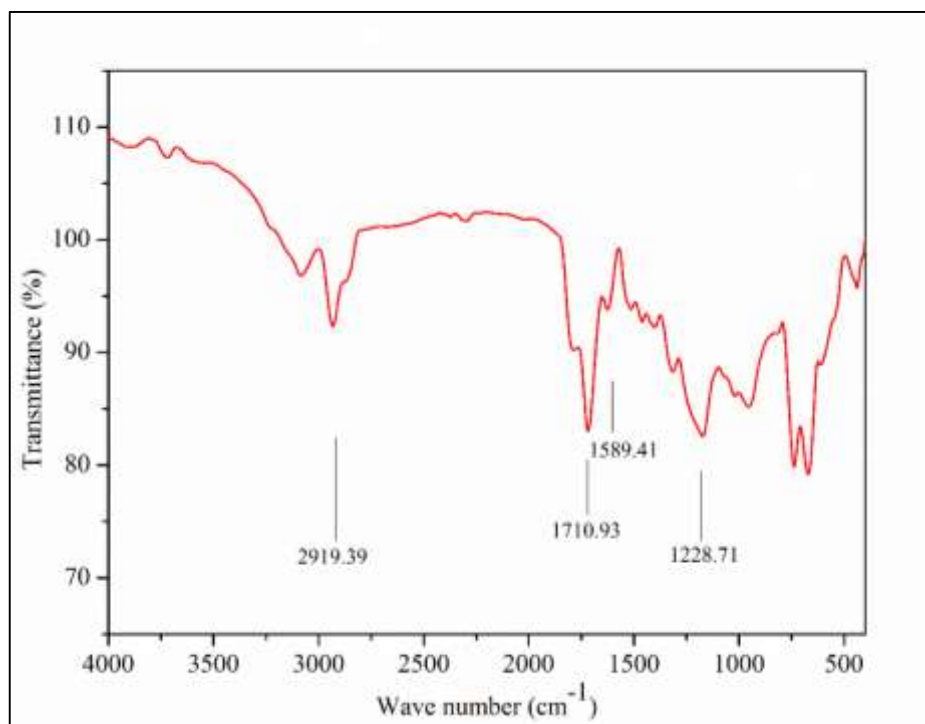


**Fig. 2.2(g) FT-IR spectrum of MPOD**

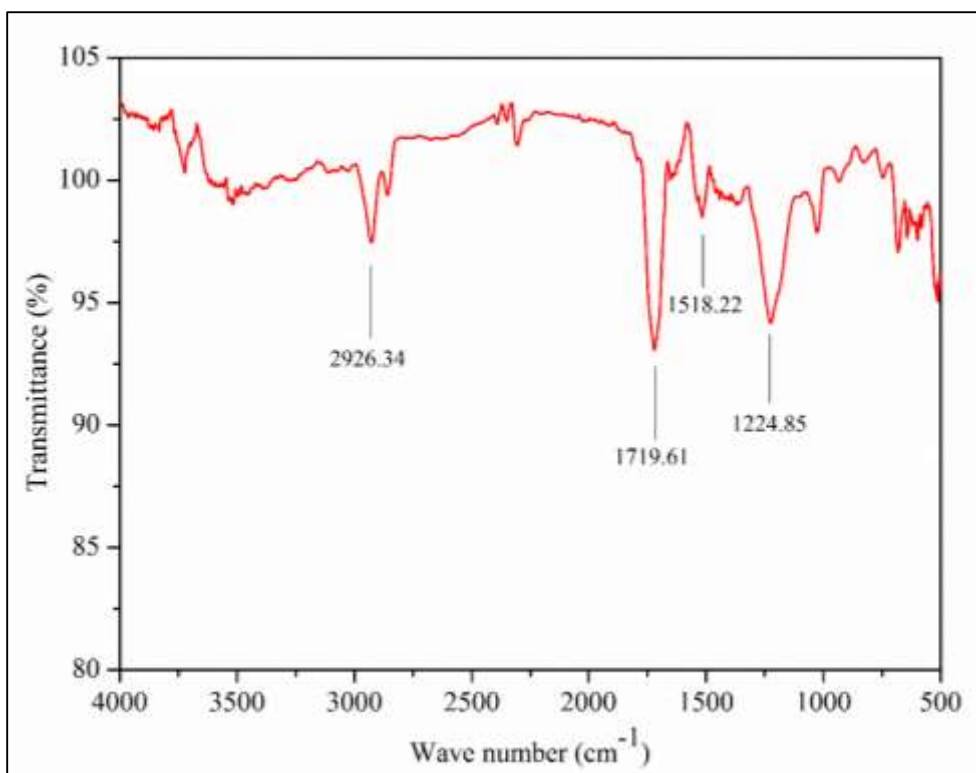


**Fig. 2.2(h) FT-IR spectrum of MPOU**

## $^1\text{H}$ NMR Spectra of aliphatic polyesters

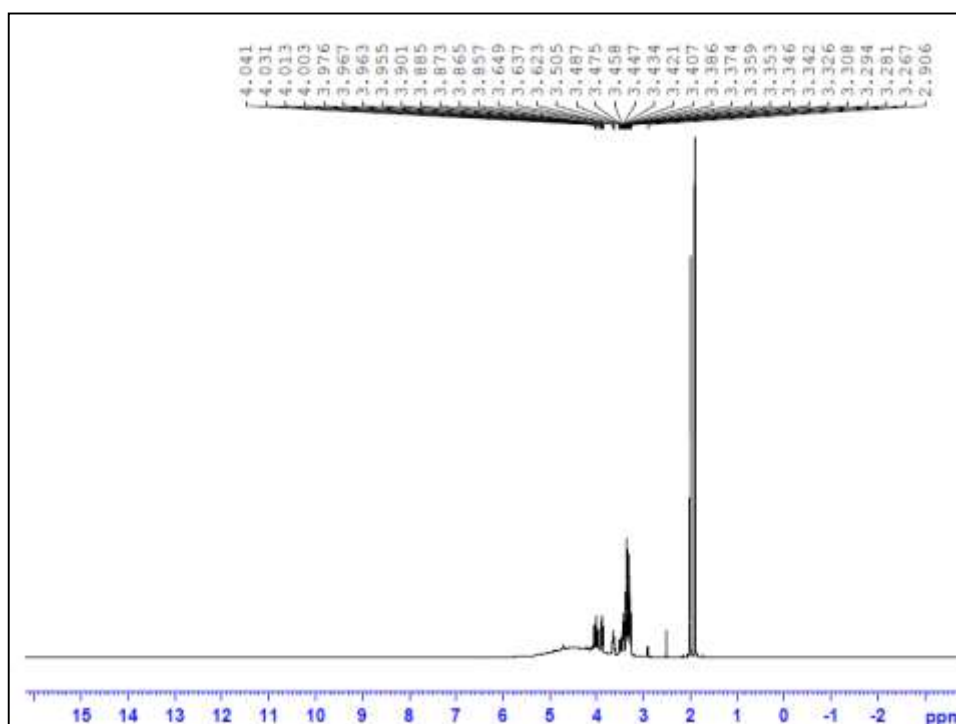


Fig. 2.3(a)  $^1\text{H}$  NMR spectrum of PGM

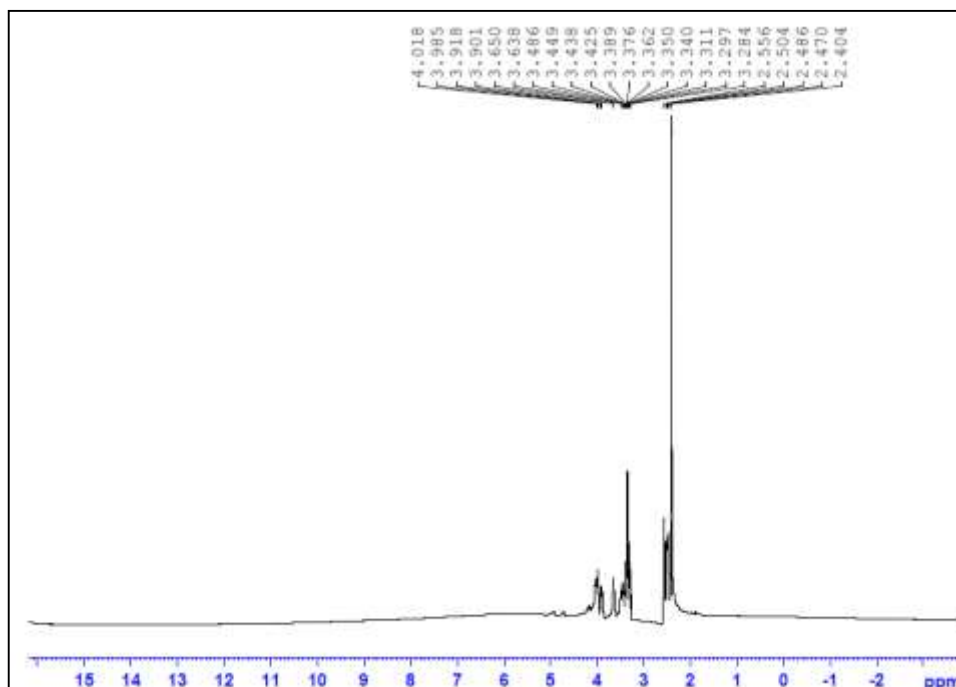


Fig. 2.3(b)  $^1\text{H}$  NMR spectrum of PGS

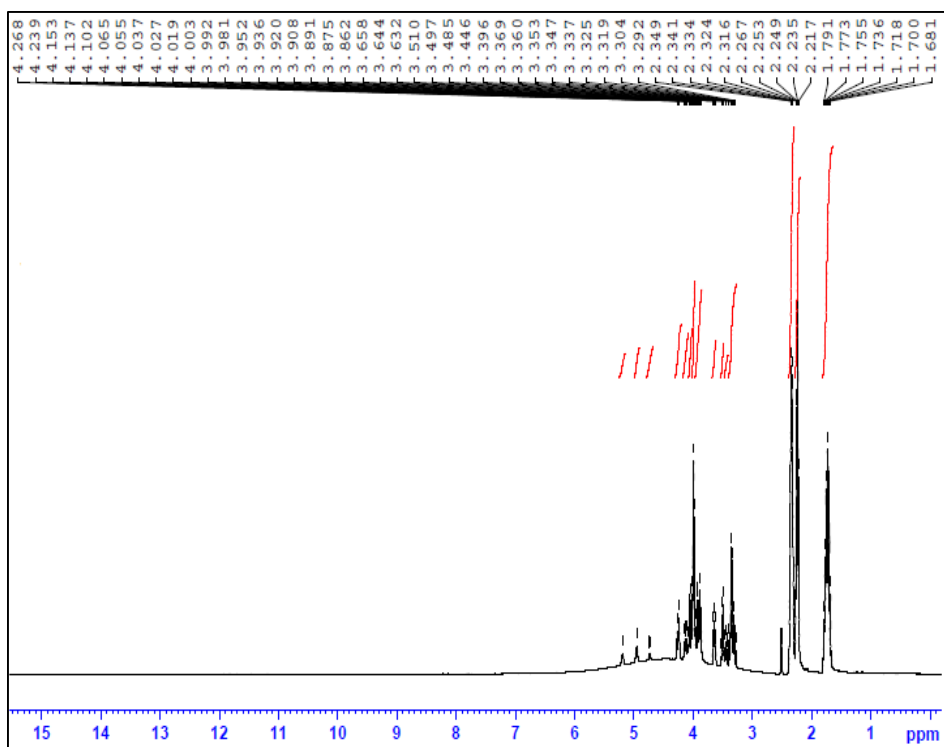


Fig. 2.3(c)  $^1\text{H}$  NMR spectrum of PGG

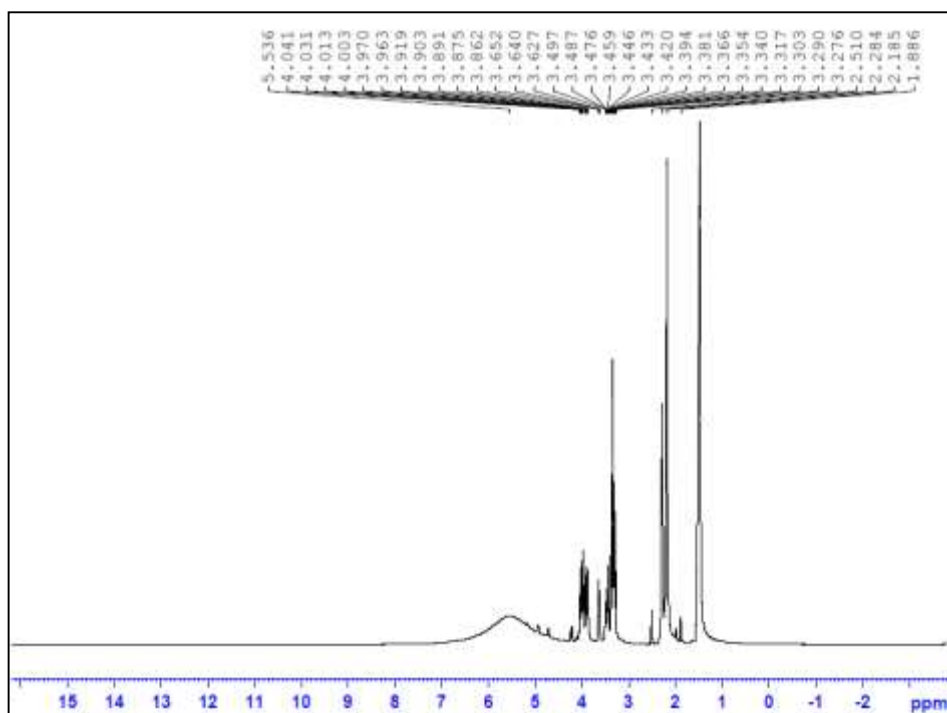


Fig. 2.3(d)  $^1\text{H}$  NMR spectrum of PGA

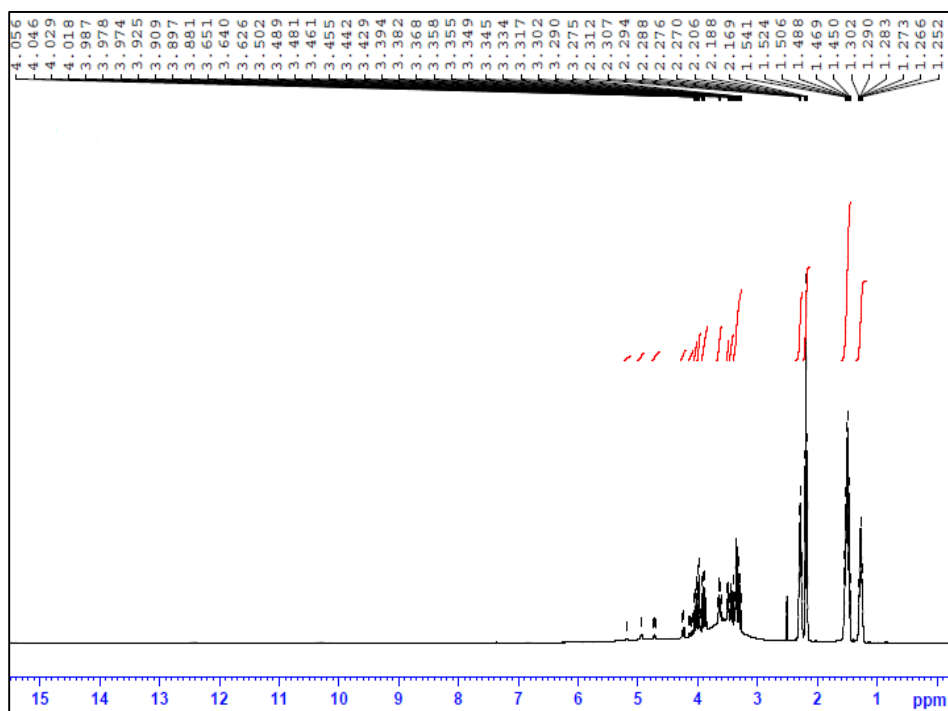


Fig. 2.3(e)  $^1\text{H}$  NMR spectrum of PGP

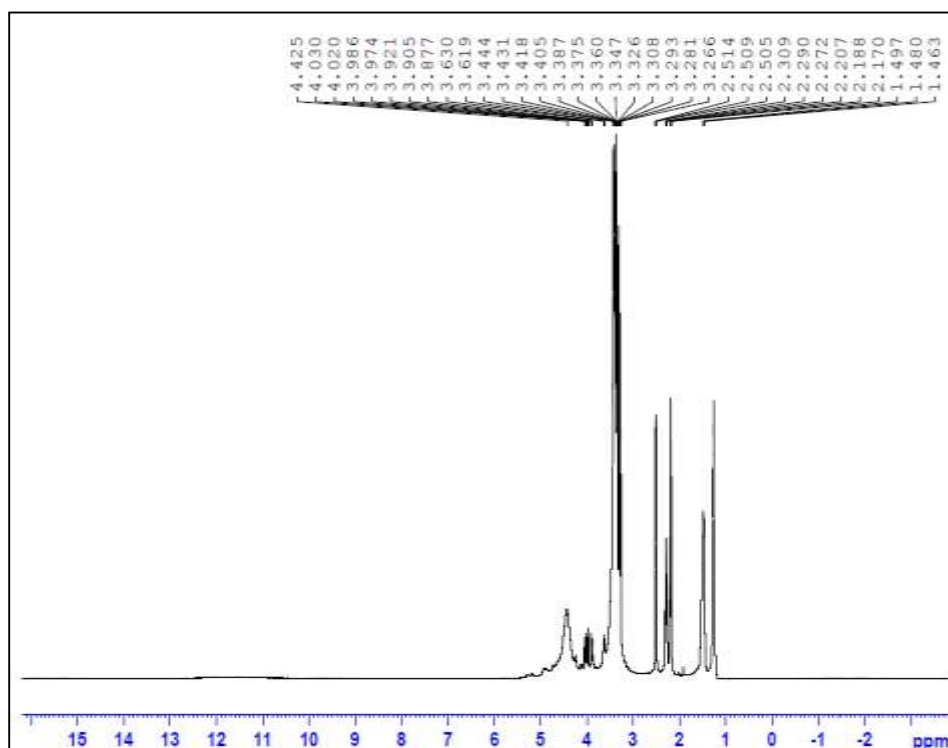


Fig. 2.3(f)  $^1\text{H}$  NMR spectrum of PGSU

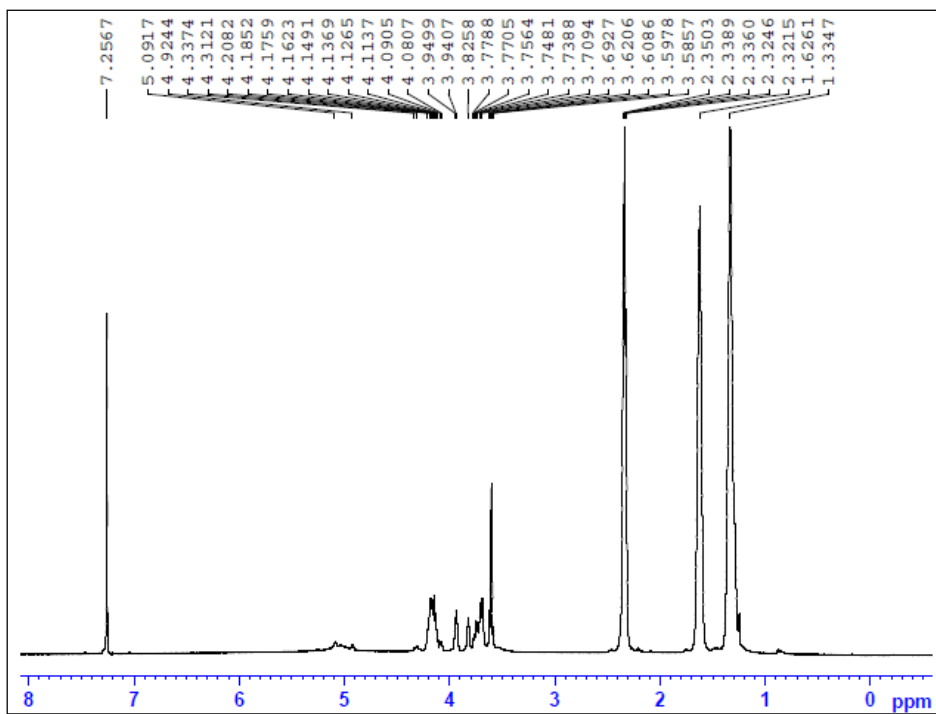


Fig. 2.3(g)  $^1\text{H}$  NMR spectrum of PGAZ

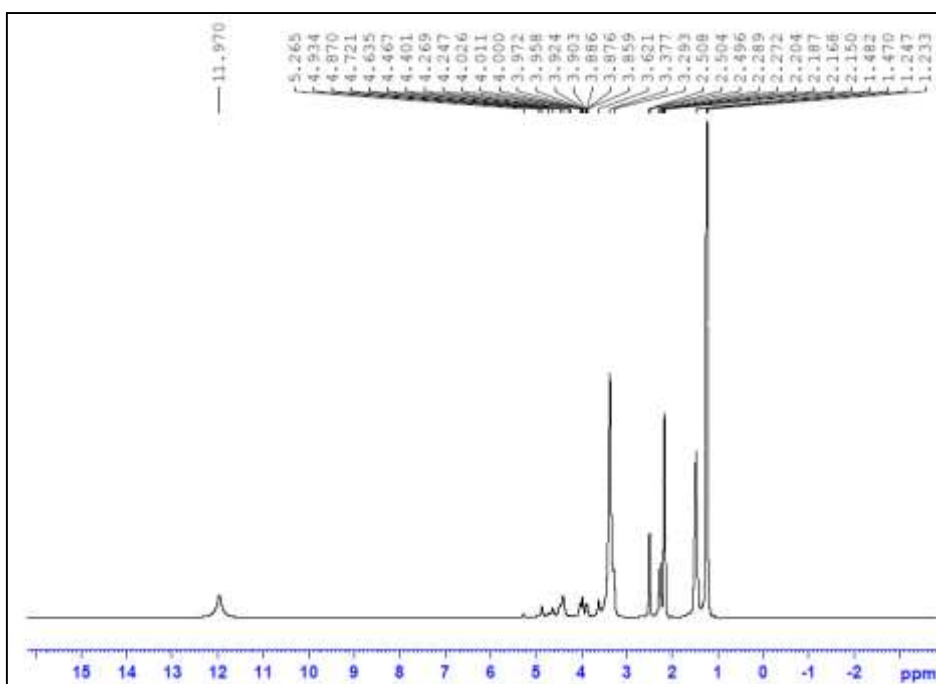


Fig. 2.3(h)  $^1\text{H}$  NMR spectrum of PGSE

## <sup>1</sup>H NMR Spectra of aromatic (cardo) polyesters

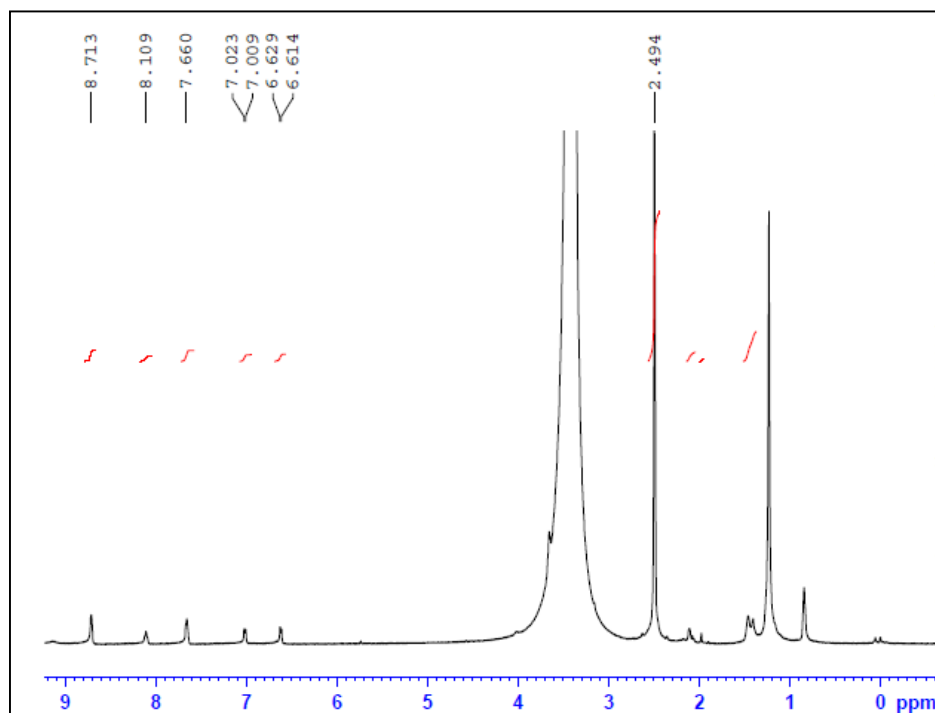


Fig. 2.4(a) <sup>1</sup>H NMR spectrum of MPOB

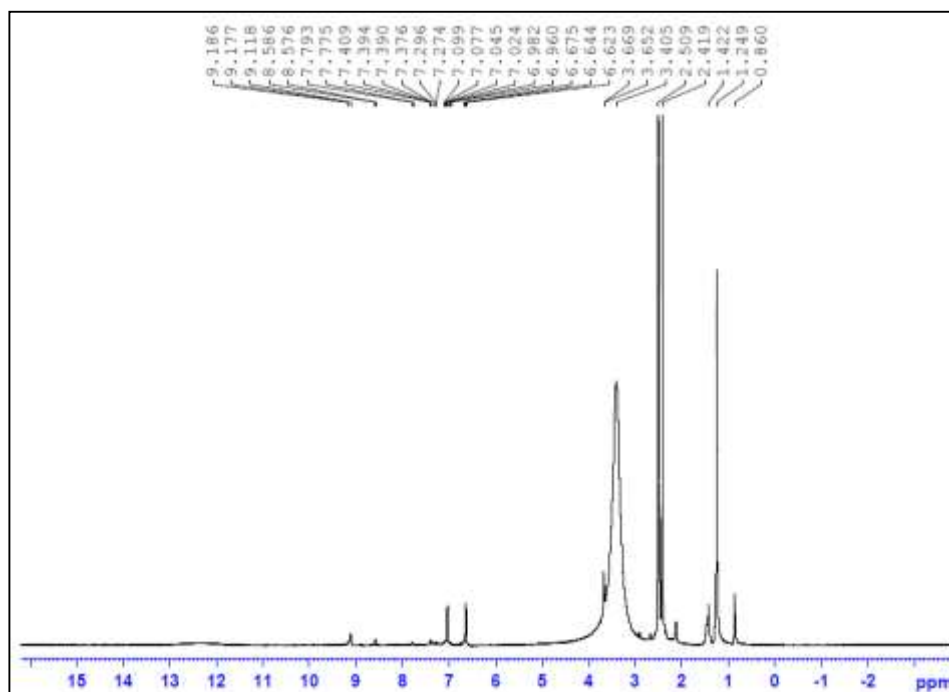


Fig. 2.4(b) <sup>1</sup>H NMR spectrum of MPOP

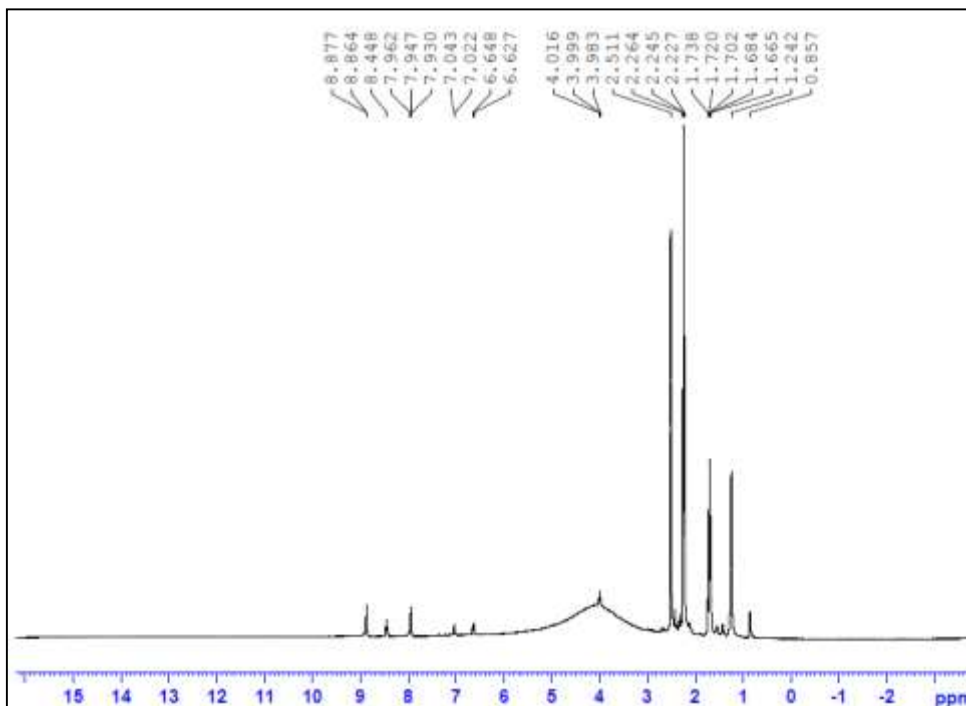


Fig. 2.4(c)  $^1\text{H}$  NMR spectrum of MPOHX

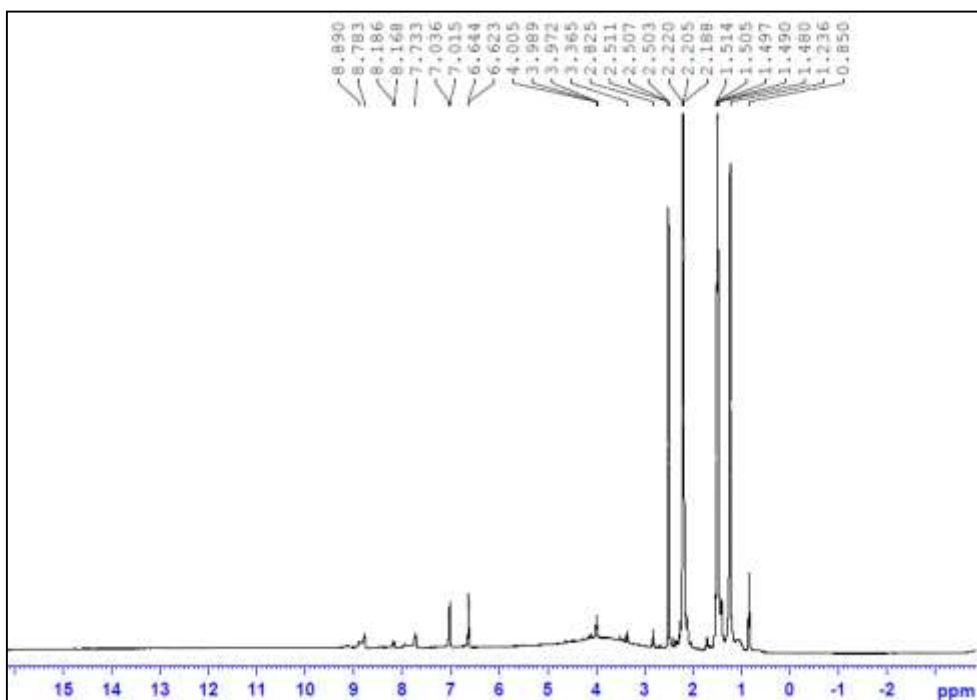


Fig. 2.4(d)  $^1\text{H}$  NMR spectrum of MPOHP



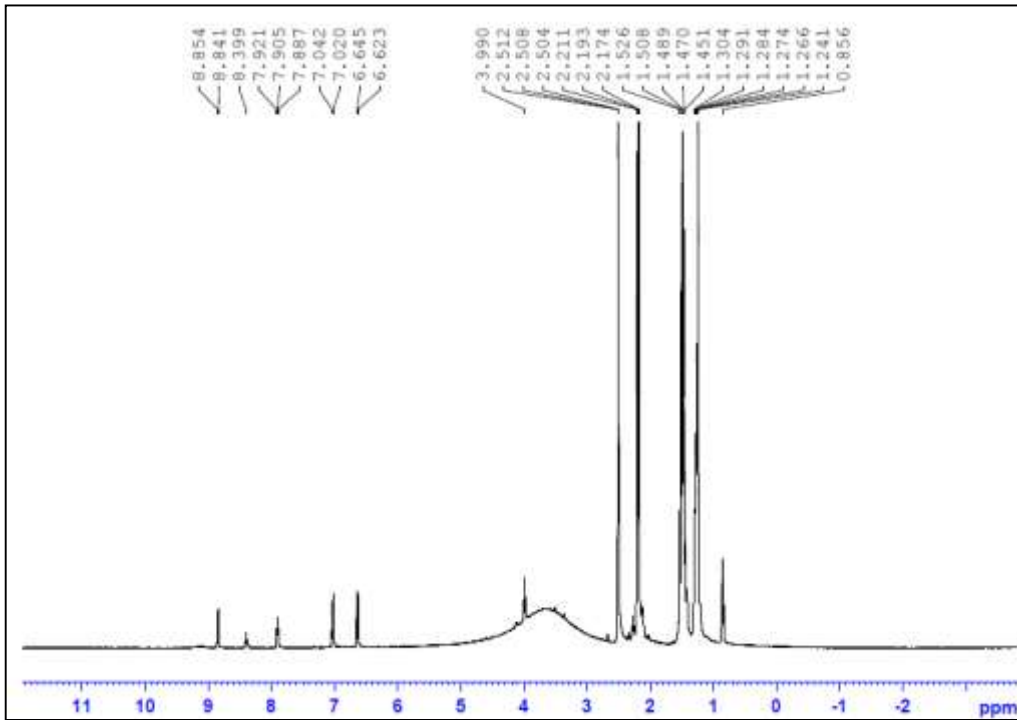


Fig. 2.4(e) <sup>1</sup>H NMR spectrum of MPOO

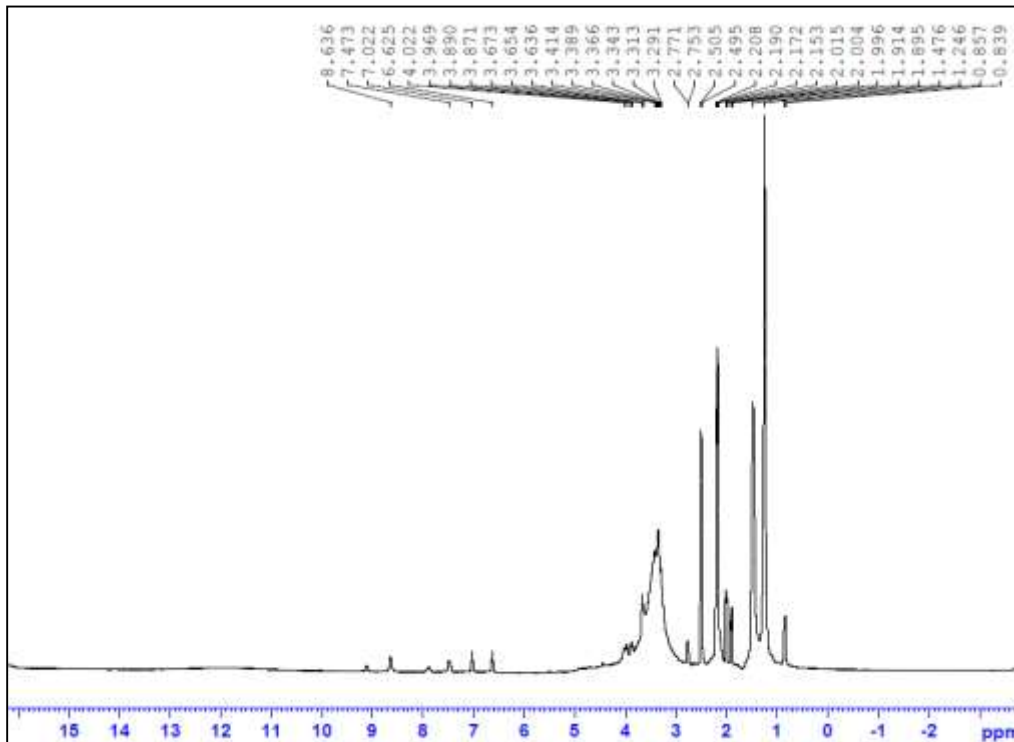


Fig. 2.4(f) <sup>1</sup>H NMR spectrum of MPON

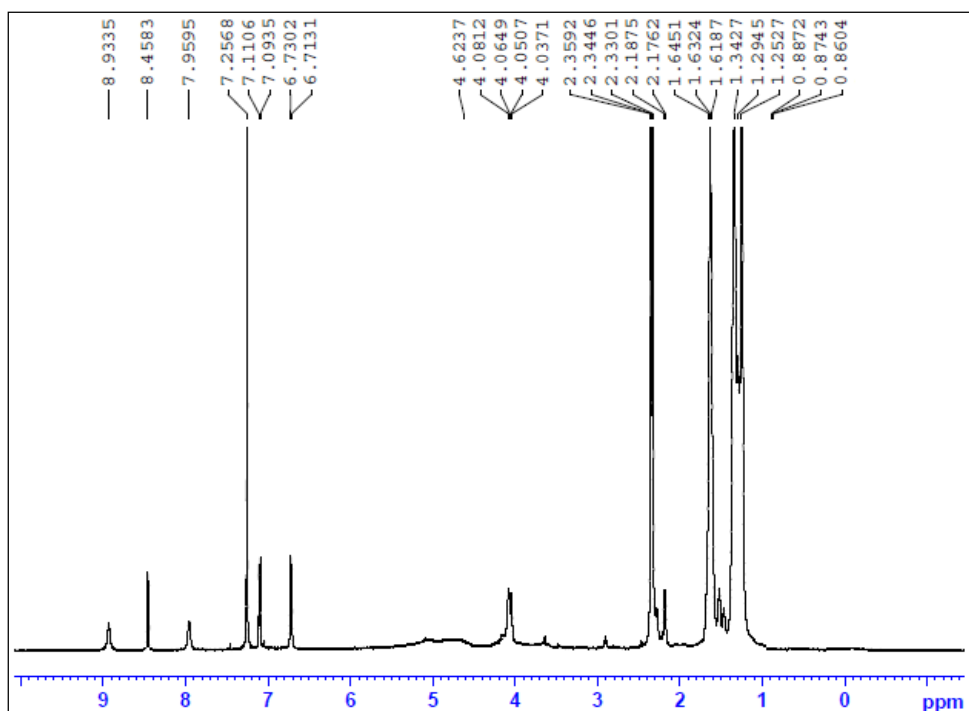


Fig. 2.4(g) <sup>1</sup>H NMR spectrum of MPOD

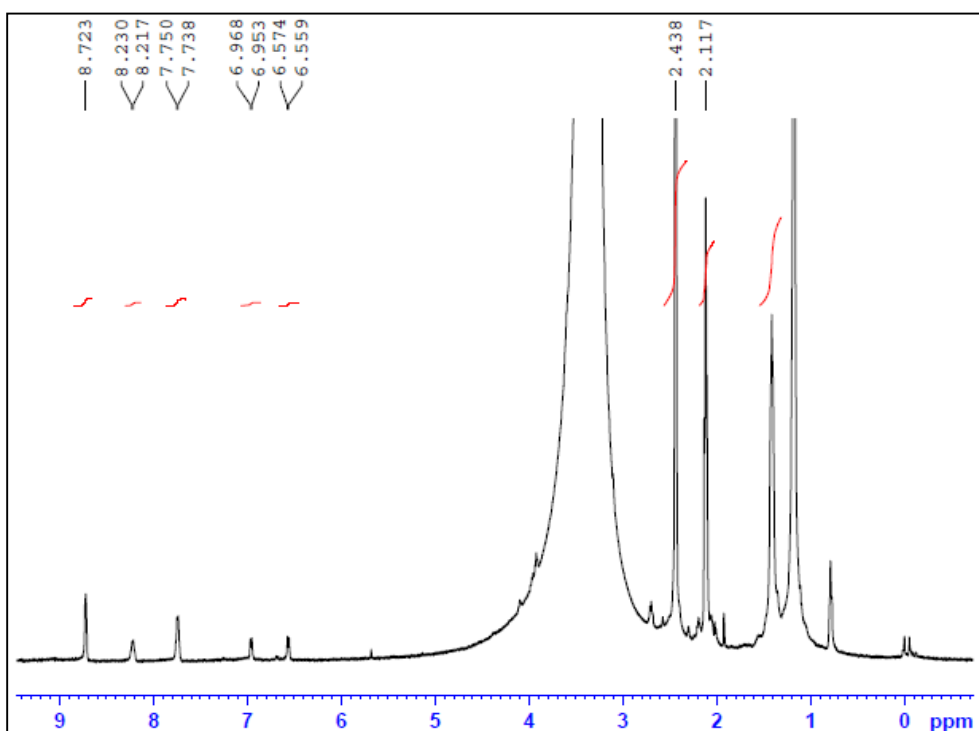


Fig. 2.4(h) <sup>1</sup>H NMR spectrum of MPOU





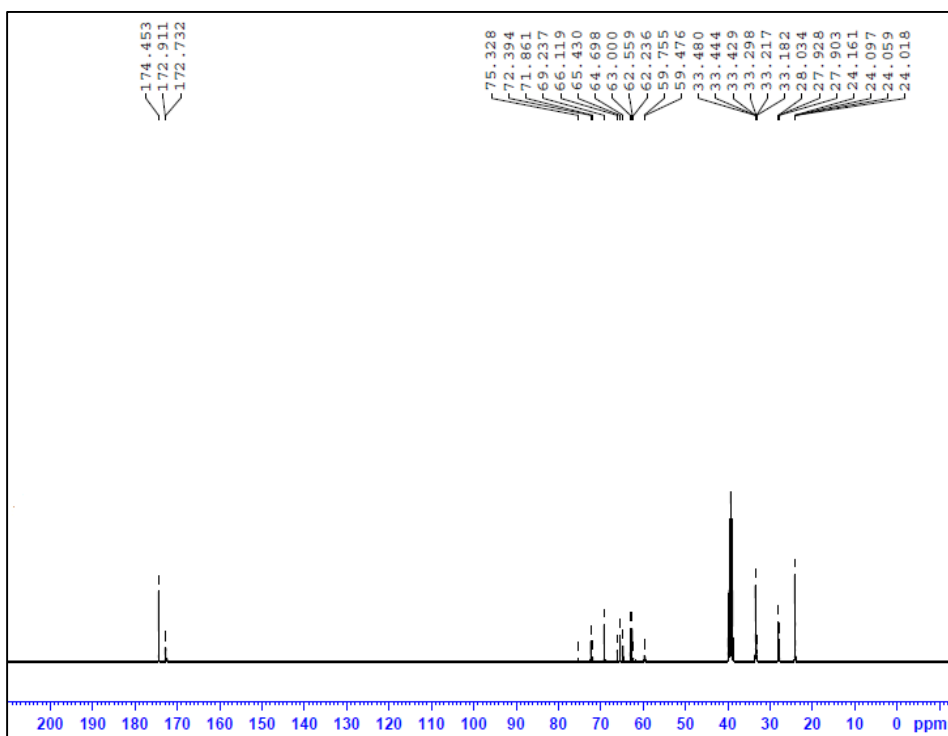


Fig. 2.5(e)  $^{13}\text{C}$  NMR Spectra of PGP

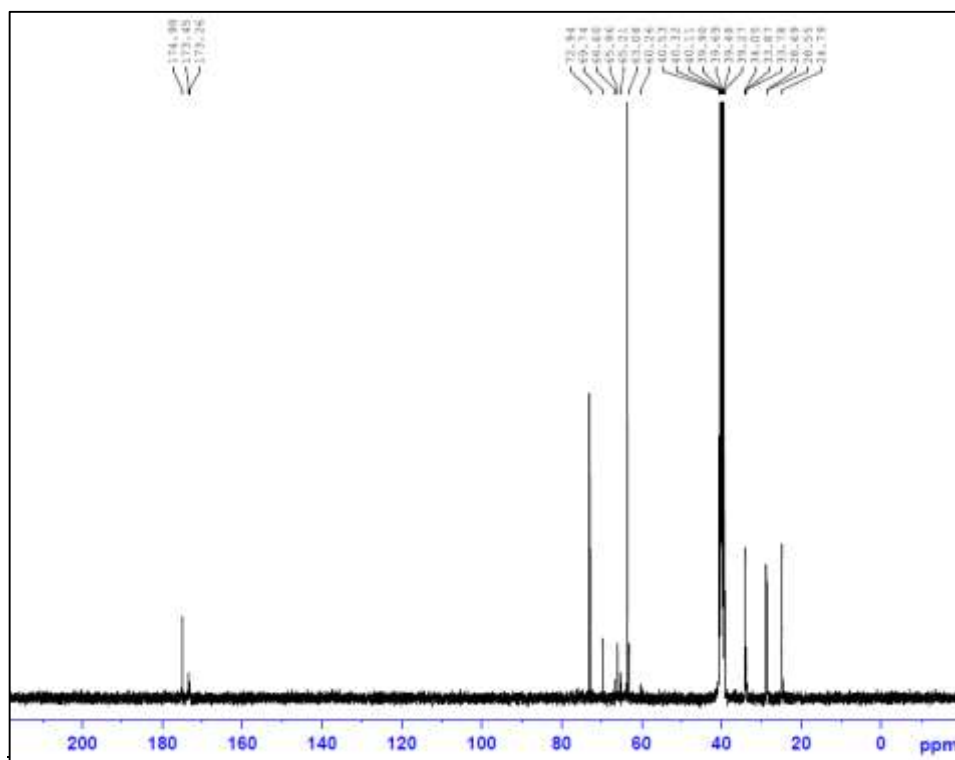


Fig. 2.5(f)  $^{13}\text{C}$  NMR Spectra of PGSU



### <sup>13</sup>C NMR Spectra of aromatic (cardo) polyesters

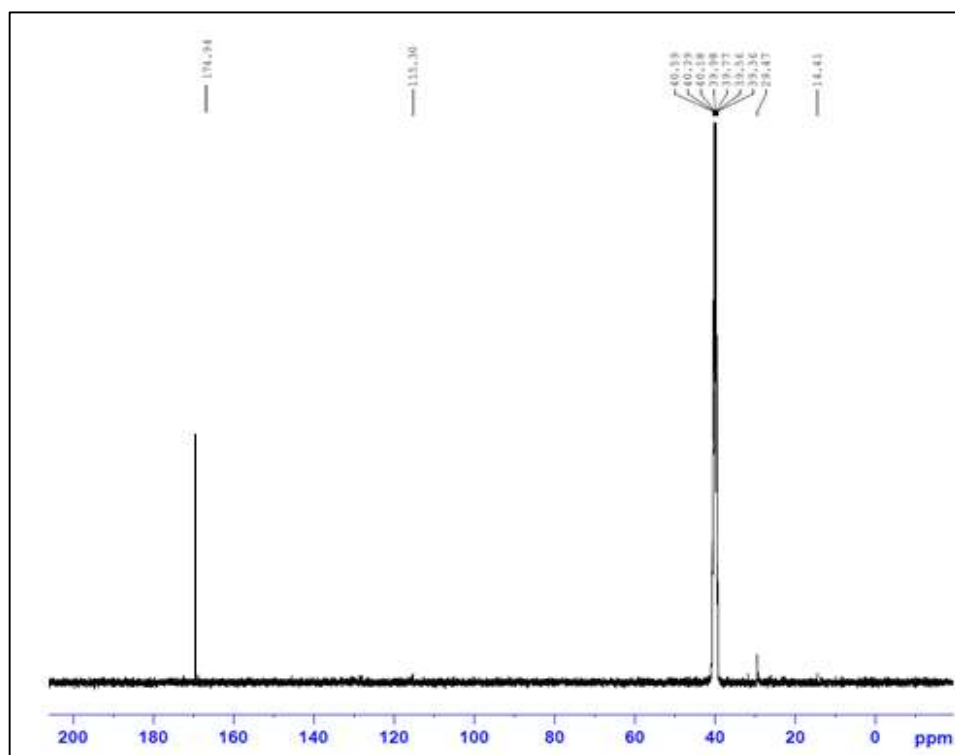


Fig. 2.6(a) <sup>13</sup>C NMR Spectra of MPOB

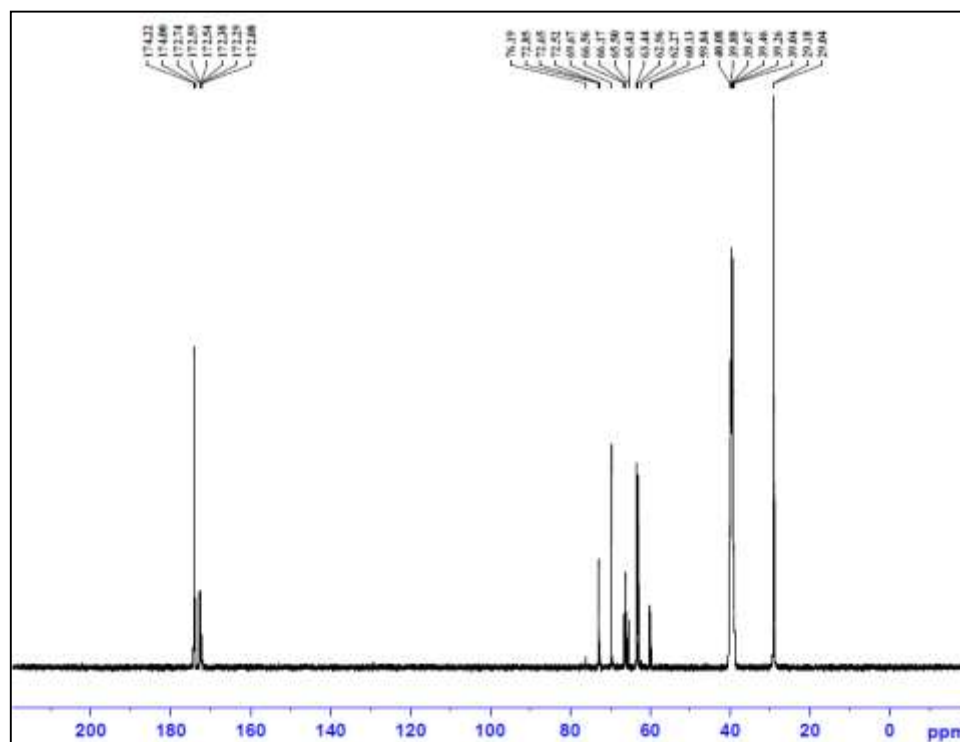


Fig. 2.6(b) <sup>13</sup>C NMR Spectra of MPOP





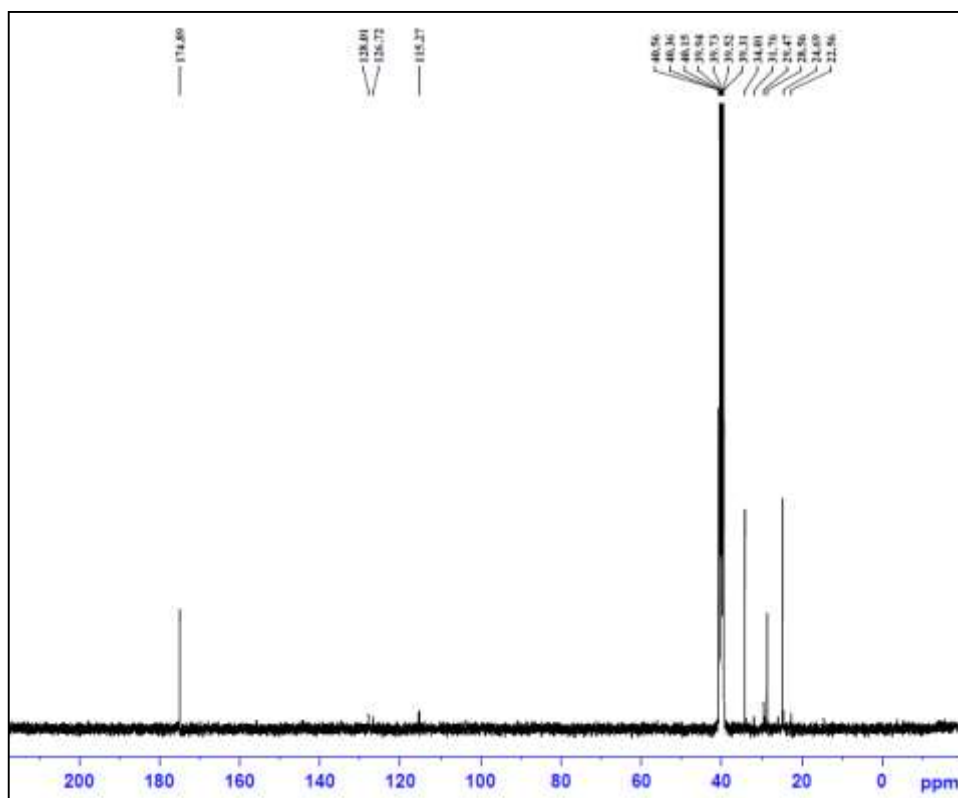


Fig. 2.6(e)  $^{13}\text{C}$  NMR Spectra of MPOO

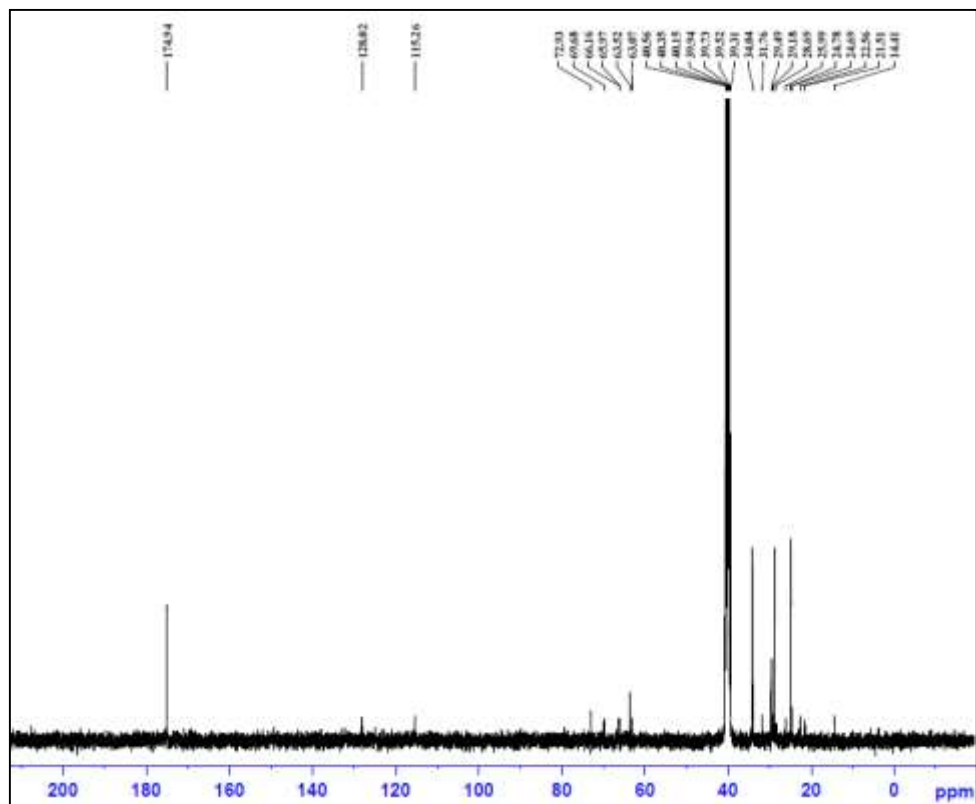
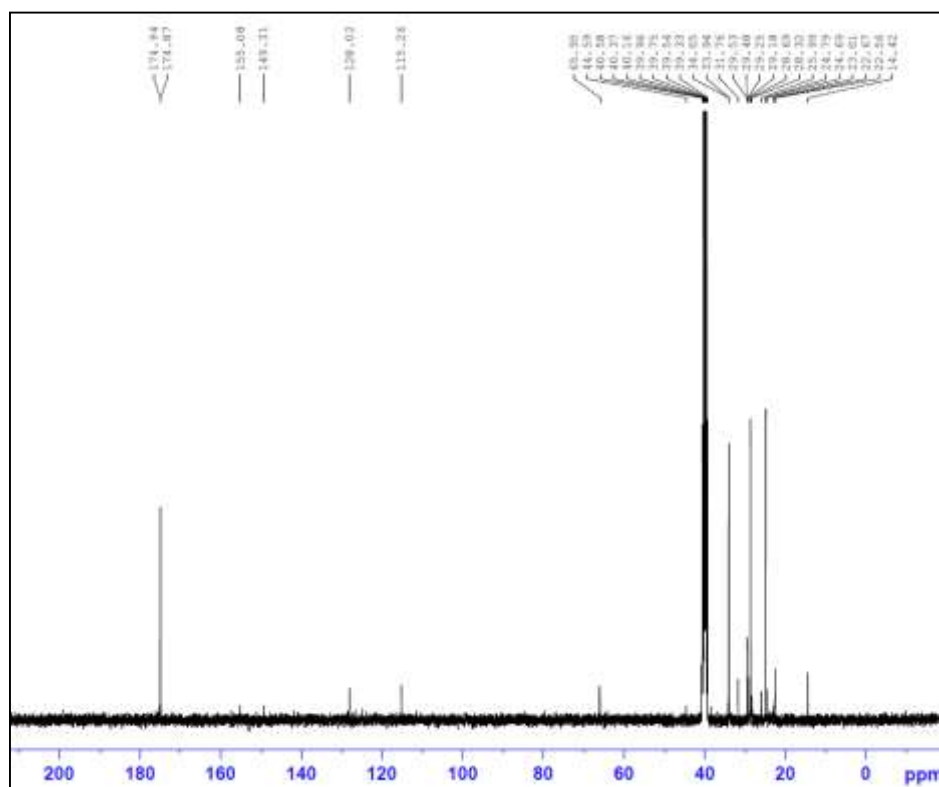
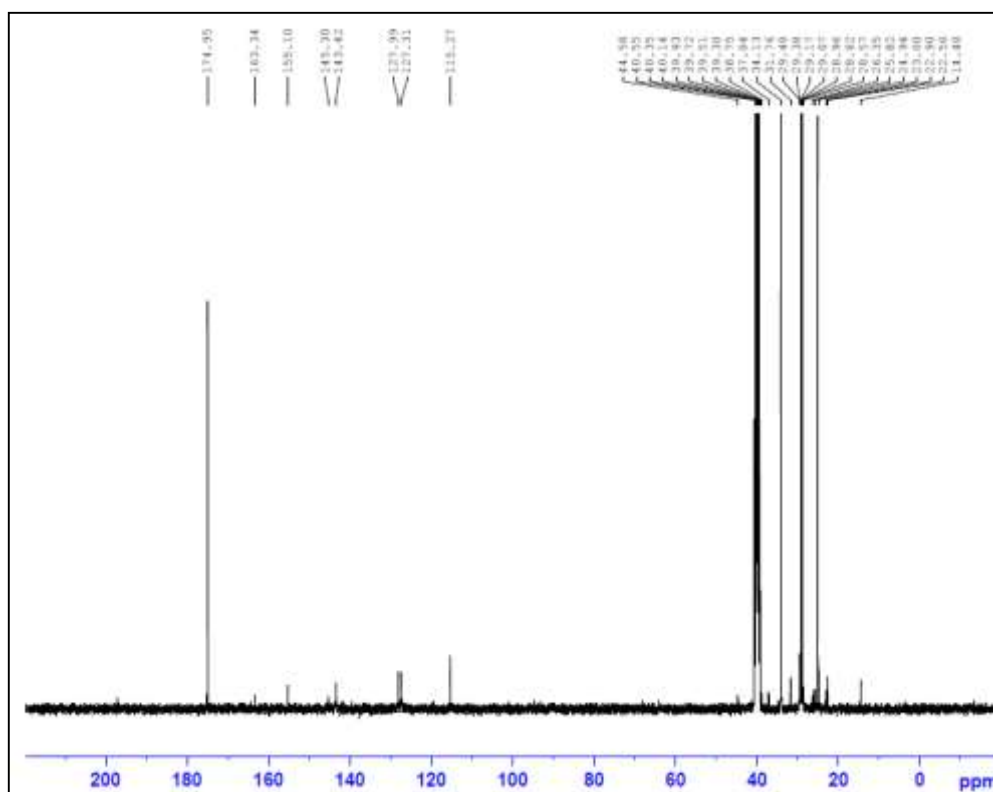


Fig. 2.6(f)  $^{13}\text{C}$  NMR Spectra of MPON

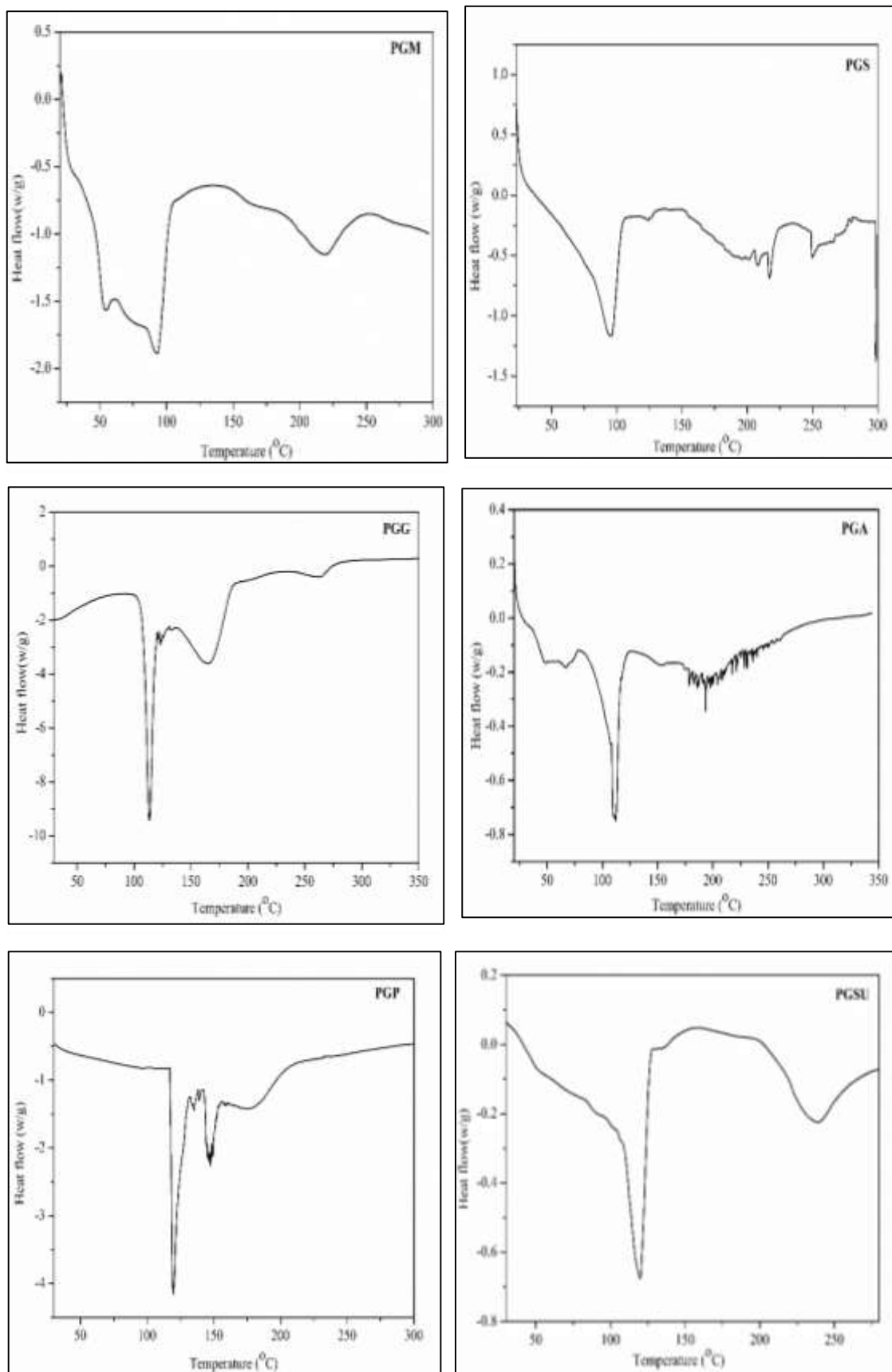


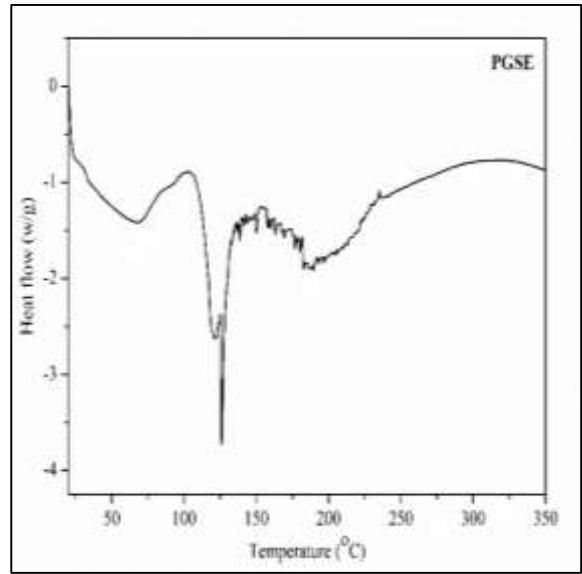
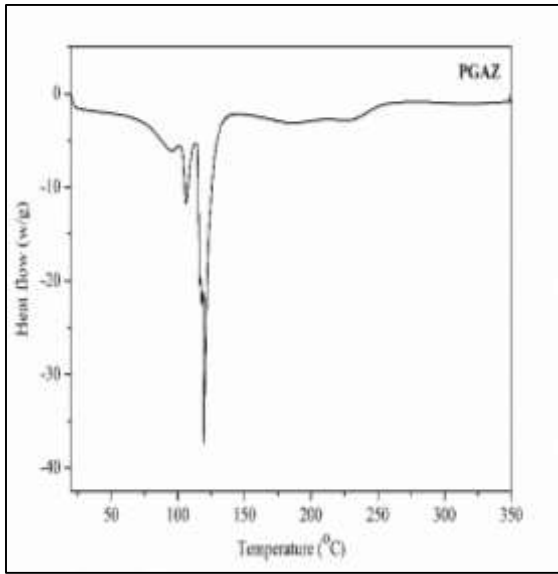
**Fig. 2.6(g)**  $^{13}\text{C}$  NMR Spectra of MPOD



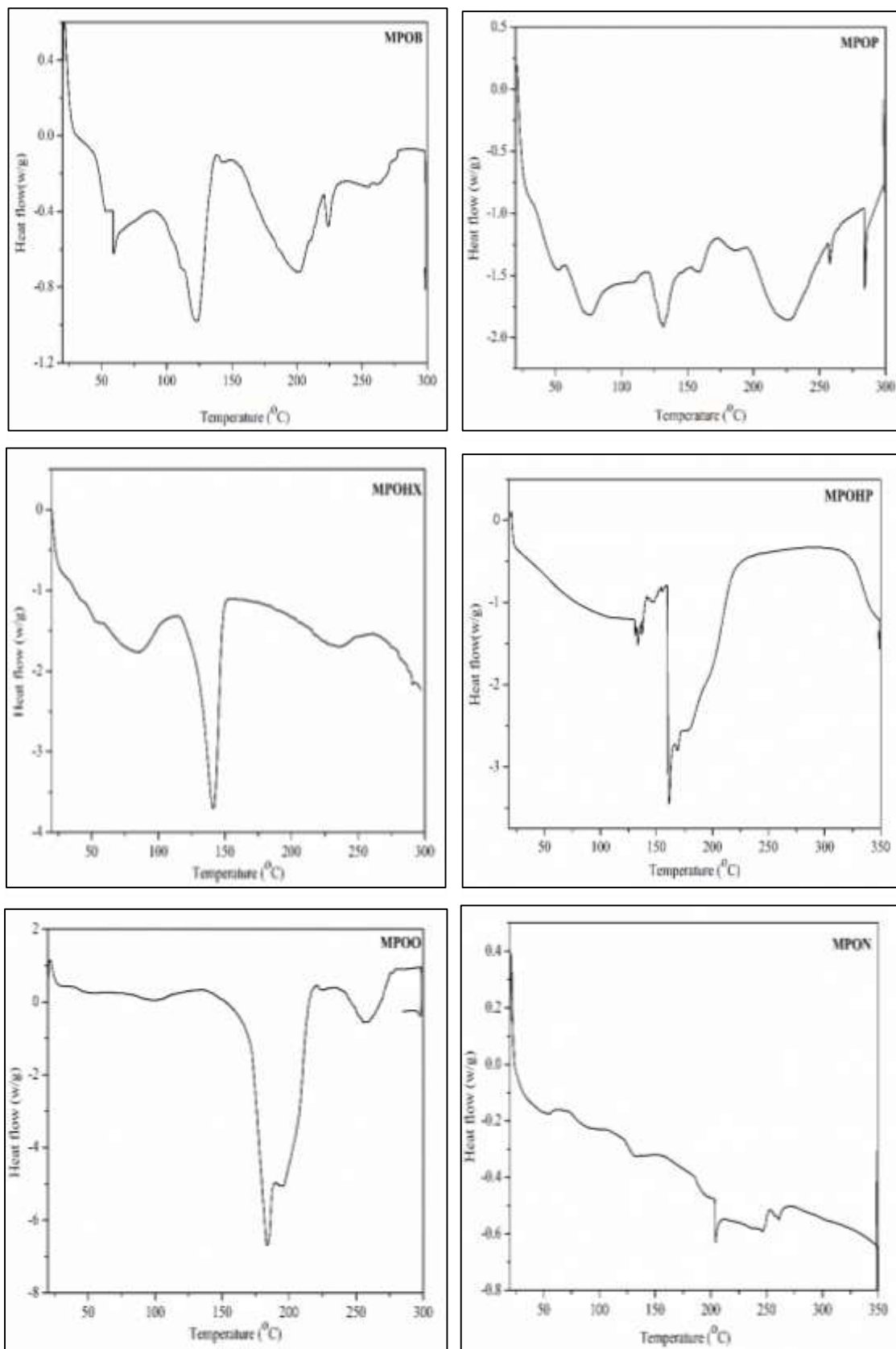
**Fig. 2.6(h)**  $^{13}\text{C}$  NMR Spectra of MPOU

Fig. 2.7 DSC thermograms of aliphatic polyesters under nitrogen atmosphere





**Fig. 2.8 DSC thermograms of aromatic (cardo) polyesters under nitrogen atmosphere**



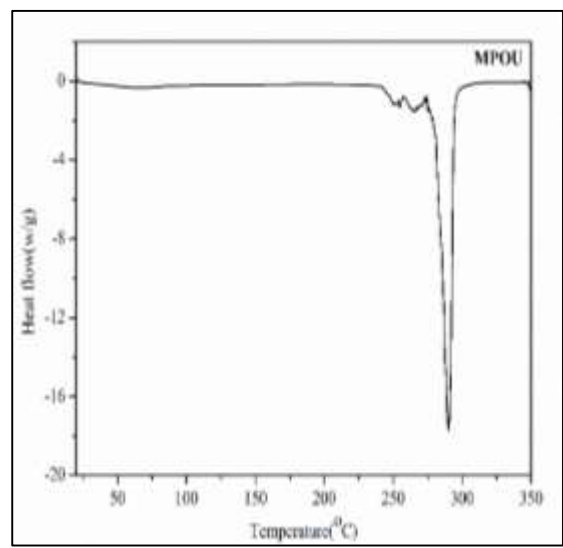
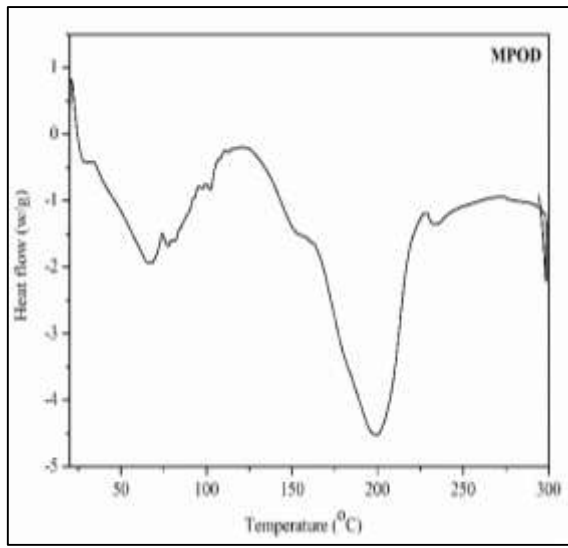
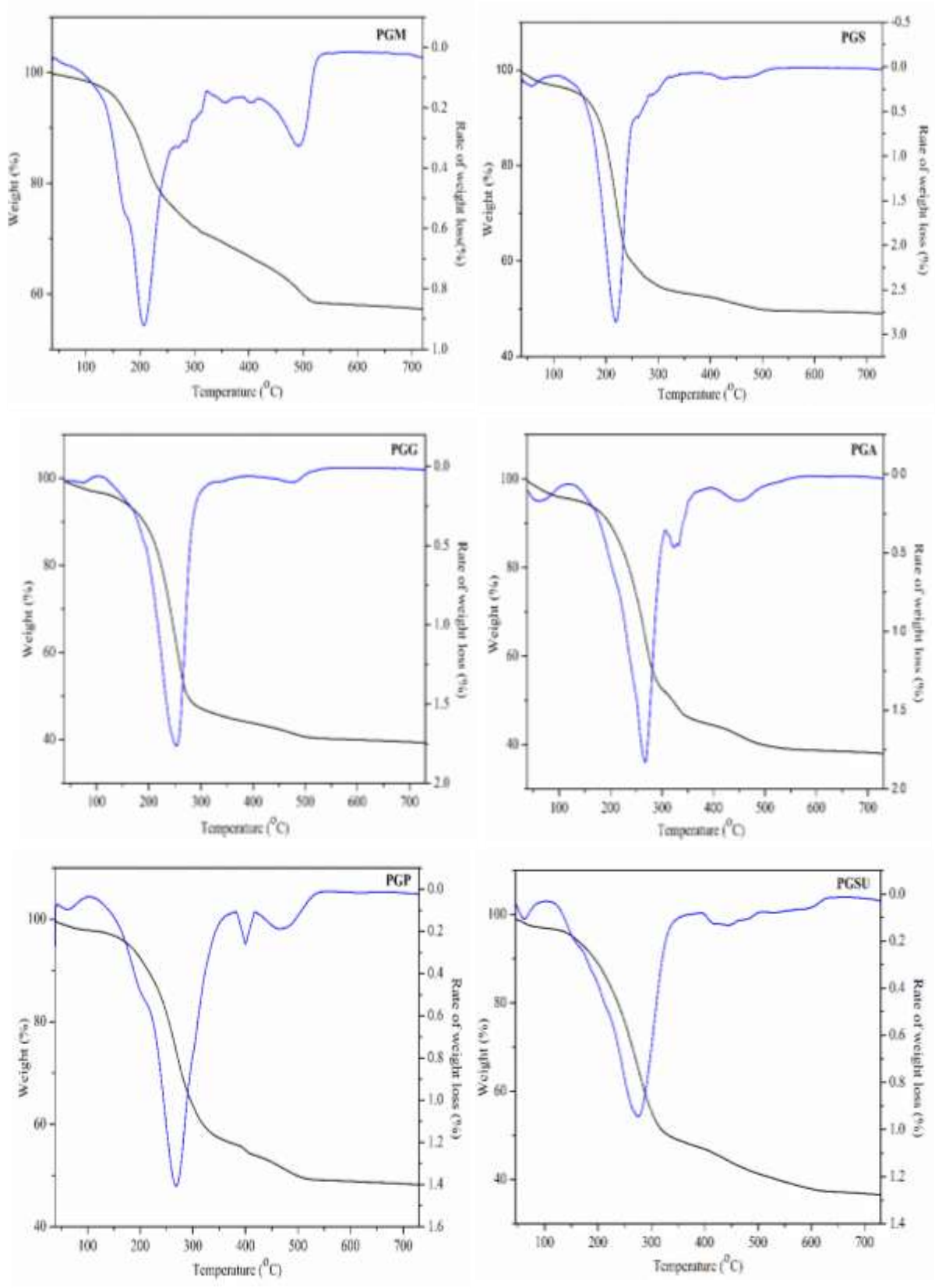


Fig. 2.9 TGA curves for aliphatic polyesters in nitrogen atmosphere



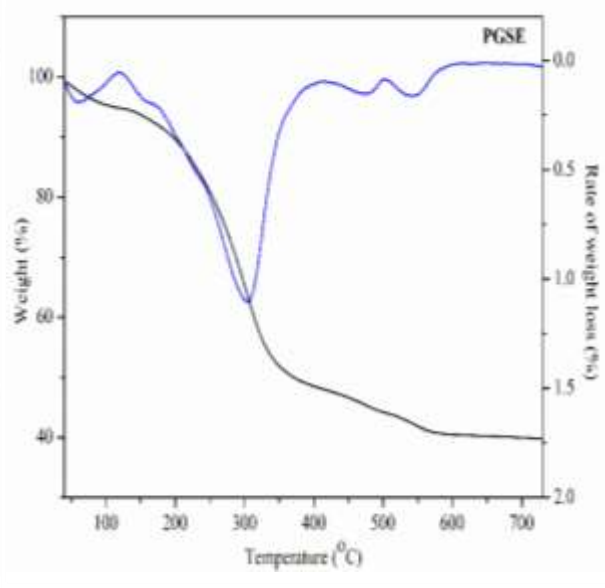
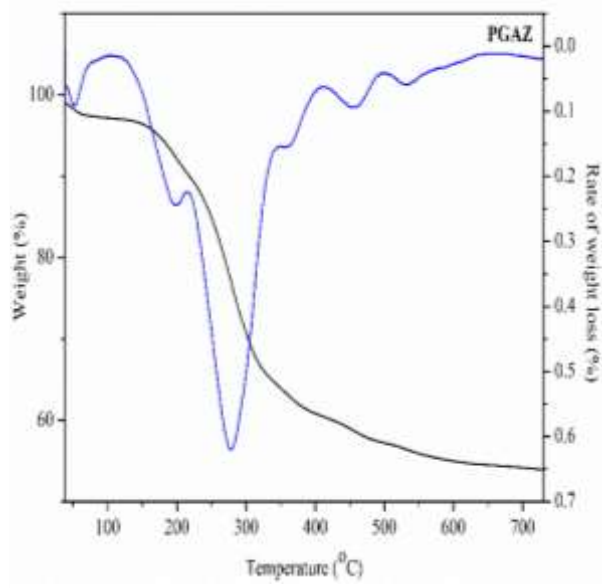




Fig. 2.10 TGA curves for aromatic (cardo) polyesters in nitrogen atmosphere

